Journal of Medicinal Chemistry

pubs.acs.org/jmc Article

Phosphinanes and Azaphosphinanes as Potent and Selective Inhibitors of Activated Thrombin-Activatable Fibrinolysis Inhibitor (TAFIa)

Arnaud-Pierre Schaffner,* Patricia Sansilvestri-Morel, Nicole Despaux, Elisabeth Ruano, Thierry Persigand, Alain Rupin, Philippe Mennecier, Marie-Odile Vallez, Eric Raimbaud, Patrice Desos, and Philippe Gloanec

Cite This: *J. Med. Chem.* 2021, 64, 3897−3910 Read Online

ACCESS | Metrics & More | Article Recommendations | Supporting Information

ABSTRACT: Selective and potent inhibitors of activated thrombin activatable fibrinolysis inhibitor (TAFIa) have the potential to increase endogenous and therapeutic fibrinolysis and to behave like profibrinolytic agents without the risk of major hemorrhage, since they do not interfere either with platelet activation or with coagulation during blood hemostasis. Therefore, TAFIa inhibitors could be used in at-risk patients for the treatment, prevention, and secondary prevention of stroke, venous thrombosis, and pulmonary embolisms. In this paper, we describe the design, the structure−activity relationship (SAR), and the synthesis of novel, potent, and selective phosphinanes and azaphosphinanes as TAFIa inhibitors. Several highly active azaphosphinanes display attractive properties suitable for further *in vivo* efficacy studies in thrombosis models.

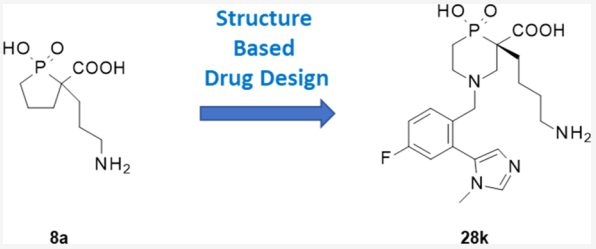

INTRODUCTION

Hemostasis is the physiological process that stops bleeding in all animals with a closed circulatory system while keeping the blood in a liquid state inside the vessels. Hemostasis takes place in three successive stages, including platelet aggregation, coagulation, and fibrinolysis. Thrombotic diseases represent one of the main causes of death in developed countries. Poor nutrition, lack of physical exertion, or even smoking are aggravating factors.

Fibrinolysis prevents the extension of the clot by destroying the fibrin polymers. Fibrinolysis is activated by the binding of tissue plasminogen activator (t-PA) (released by activated endothelial cells) on the C-terminal lysine residues of fibrin, which are high affinity receptors for t-PA. This t-PA binding allows the enzymatic activation of the circulating plasminogen into the proteolytic enzyme, plasmin, which breaks down the fibrin clots. The fibrinolytic system balances breakdown of intravascular clots formed following coagulation and prevention of hemorrhages by premature dissolution of hemostatic clots. Thus, fibrinolysis is a highly regulated process in which endogenous fibrinolysis inhibitors slow down the fibrin breakdown. Among these inhibitors, the carboxypeptidase (CP) TAFIa, activated thrombin activatable fibrinolysis inhibitor, resulting from the activation of the TAFI zymogen, acts on fibrinolysis by cleavage of C-terminal lysine residues on the surface of fibrin, preventing plasmin generation by t-PA. TAFI is expressed as a 55 kDa protein synthesized primarily in the liver. It circulates in the plasma in a form of zymogen. TAFIa is activated by the thrombin/thrombomodulin (TM) enzyme complex or by plasmin.[6]

TAFIa constitutes an important negative regulation of fibrinolysis. A low level of TAFI has been associated with chronic liver disease and an increased risk of bleeding.[1] On the other hand, high concentrations are correlated with an increased risk of thrombosis, coronary artery disease due to less fibrinolytic activity. Furthermore, it has been described that venous thrombosis and thromboembolism risks are associated with increased plasma levels of TAFIa in patients.[2] The implication of TAFIa in thrombosis diseases has been demonstrated in preclinical models. In knock out (KO) mice, thrombus size and weight are reduced following $FeCl_3$-induced thrombosis[3] and clot lysis is increased in a thromboembolism.[4,5] In recent years, consistent data have been obtained in animal studies on the value of TAFIa inhibitors as therapy for thrombolysis.[6] Indeed, current treatments which include thrombolytics (recombinant t-PA), antiplatelet agents, and anticoagulants present a high risk of bleeding which might be lesser with a TAFIa inhibitor treatment.

Received: November 29, 2020
Published: March 25, 2021

Downloaded via UNIV OF CONNECTICUT on May 15, 2021 at 09:09:08 (UTC).
See https://pubs.acs.org/sharingguidelines for options on how to legitimately share published articles.

ACS Publications © 2021 American Chemical Society

https://doi.org/10.1021/acs.jmedchem.0c02072
J. Med. Chem. 2021, 64, 3897−3910

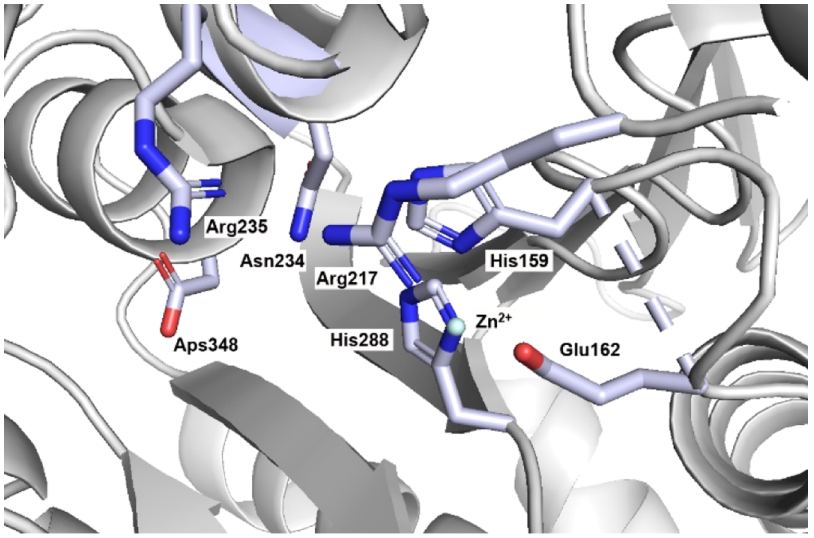

Figure 1. Holo crystal structure of human TAFI (PDB code 3D68).

TAFIa acts on fibrinolysis by cleavage of C-terminal lysine residues on the surface of fibrin, preventing plasmin generation by t-PA. The active site of TAFIa comprises the amino acids: His159, Glu162, and His288 for the coordination of Zn^{2+} and the charged residues Asp348, Arg235, and Arg217 for the anchoring of the C-terminal lysine peptide substrate.[7] The penta-coordinated zinc interacts simultaneously with the carbonyl of the substrate and a water molecule which is essential for hydrolysis (Figure 1).

RESULTS

It is well established in the literature that three main functions are necessary for the recognition by TAFIa of an inhibitor including a carboxylic acid function forming intramolecular salt bridges with two arginine residues (Arg217 and Arg235), a zinc-coordinating group, and a basic moiety forming a salt bridge with Asp348.[22] The carboxylic acid and the basic function (amine) are usually separated by a 4−5 atom flexible chain (Figure 2).

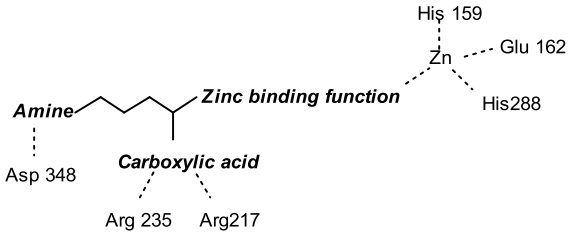

Figure 2. General pharmacophore for TAFIa inhibitors.

TAFIa inhibitors described in the literature have various zinc-chelating groups including imidazoles,[8] thiols,[9−11] carboxylic acids,[12] selenols,[13] phosphinic acids,[14,15] sulfamides,[16] and ureas.[17] To design our new inhibitors, we selected phosphinic acid as a zinc binding motif and we hypothesized that its incorporation in a cycle should reduce the conformational flexibility and consequently increase the selectivity with respect to other CPs. Indeed, other CPs such as circulating carboxypeptidase N, which plays an important role in the degradation of anaphylatoxins and kinins, are constitutively active and should not be targeted.[18] This greater rigidity should be reinforced by the presence of a quaternary carbon bearing a carboxylic acid function and an amino side chain of length to be determined. To verify these hypotheses, a preliminary series of cyclic phosphinanes were then designed by varying the length of the basic chain as well as the size of the cycle, prioritized by docking using the crystal structure of human TAFI crystallized with arginine as a ligand (PDB 3D68, Figure 3) and synthesized according to the general synthetic

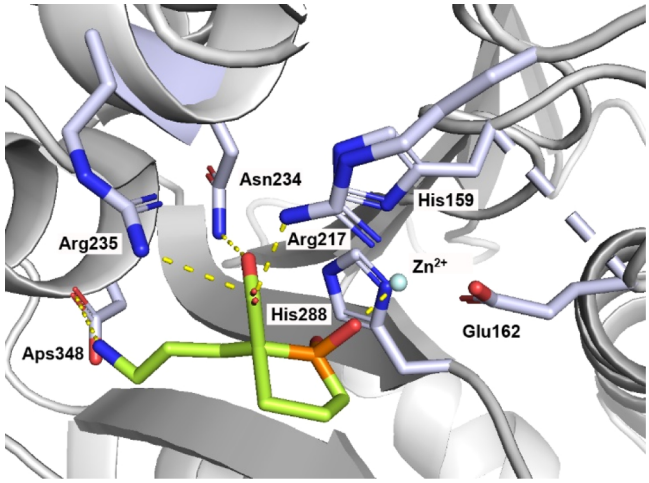

Figure 3. Docking representation of **8a**, highlighting the key interactions with TAFI.

pathway shown in Scheme 1. In its docked complex, as shown in Figure 3, **8a** maintaining the key interactions of the carboxylate with Arg217, Asn234, and Arg235, the phosphinane formed a strong interaction with the Zn^{2+} ion according to the docked structure. The terminal basic group also interacted with Asp348, although their distance of 4.1 Å suggests that use of a longer linker might be beneficial.

The bromoalkylphosphinates **2a−d** were obtained in good yields *via* an esterification/hydrophosphinylation reaction as described by Montchamp.[19] The phosphinate ethyl ester intermediate was generated *in situ* by treatment of an aqueous solution of hypophosphorous acid with an equivalent of tetraethylorthosilicate. The hydrophosphinylation was then

https://doi.org/10.1021/acs.jmedchem.0c02072
J. Med. Chem. 2021, 64, 3897−3910

Scheme 1. General Synthetic Scheme of Cyclic Phosphinane 8, Inhibitors of TAFIa[a]

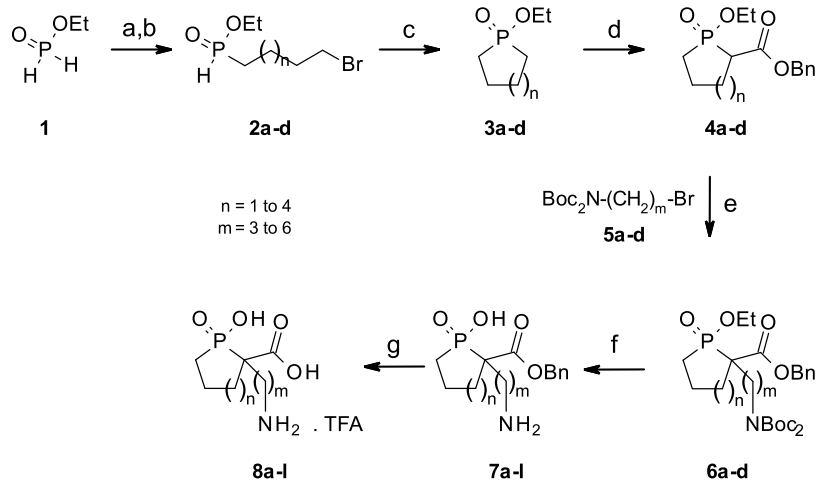

[a]Reagents and conditions: (a) tetraethylorthosilicate, MeCN, 80 °C, 2 h; (b) ω-bromoalkene, Pd_2dba_3, xantphos, MeCN, reflux, 18 h; (c) LiHMDS, THF, −78 °C; (d) LDA, DBC, THF, −70 °C, 2 h; (e) **5a−d**, NaH, DMSO, 10 °C; (f) TMS-Br, DCM, 0 °C, 20 h; (g) 10% Pd/C (10 mol%), MeOH, 20 °C, 20 h.

carried out by adding the corresponding ω-bromoalkenes in the presence of Pd_2dba_3 and Xantphos. The intramolecular alkylation allowing the formation of the corresponding cyclic phosphinanes **3a−d** was performed using LiHMDS in THF. It is important to notice that the synthetic difficulties increase with the size of the ring, and the 9-membered ring was isolated in only 1% yield. **3a−d** were then benziloxycarbonylated with dibenzylcarbonate and LDA while keeping the temperature of the mixture below −65 °C to avoid decarboxylation and led to **4a−d** as a mixture of four diastereoisomers. Different basic side chains **5a−d** were then introduced by alkylation using NaH in DMSO at room temperature to give **6a−l**. The simultaneous hydrolysis of the phosphinate ethyl ester and of the two *tert*-butoxycarbamate groups was performed using trimethylsilyl bromide and followed by methanolysis of the intermediate silylated esters to afford **7**. Finally, after hydrogenolysis, the target compounds **8a−l** were isolated as racemic mixtures in nearly quantitative yields.

These compounds were then tested for their ability to inhibit human activated TAFI. Briefly, purified recombinant human TAFI was activated by thrombin/thrombomodulin to generate TAFIa. Compounds were incubated with the protein, and hippuryl-arginine was added. The ability of compounds to dose dependently decrease the formation of hippuric acid (product of the reaction) was evaluated, and IC_{50} were calculated (Table 1).

Although the five membered phosphinanes (n = 1) were typically weak inhibitors of TAFIa, we observed a preference for the longer linkers (**8b**, **8c**). Moving to the larger rings (n > 1), this trend was recapitulated, suggesting that the chain with three carbon atoms is too short to establish interaction with Asp348. On comparing the effect of the chain length on the TAFIa inhibition for the larger phosphinane cycles (n = 2−4), the most promising results were obtained with a chain of C5 (**8f**, **8i**, and **8k**). The increase in ring size appears to improve the affinity as illustrated with **8k** and its 8-membered ring, which represented the most active TAFIa inhibitor so far (IC_{50} = 1.1 μM). Further increase of the ring size (n = 5) in combination with the optimal linker length (m = 5) led to no further improvement (**8l**). The data in Table 1 suggest that we have reached a plateau of potency in this series. Therefore,

Table 1. Inhibition of Human Activated TAFI by Cyclic Phosphinanes 8a−l

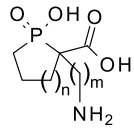

8a-l

compounds	n	m	IC_{50} hTAFIa (μM)
8a	1	3	>30.0
8b	1	4	19.0
8c	1	5	18.0
8d	2	3	>30.0
8e	2	4	11.7
8f	2	5	5.0
8g	2	6	>30.0
8h	3	4	5.0
8i	3	5	1.8
8j	4	4	2.6
8k	4	5	1.1
8l	5	5	1.5

other modifications were required to increase the affinity of these inhibitors. Analysis of the docked structure of **8a** (Figure 3) suggested that the incorporation of a nitrogen atom in the cycle could lead to the formation of a salt bridge with the side chain of Glu363. Docking of the *N*-benzyl-azaphosphinane **14d** into TAFI (derived from PDB 3D68, Figure 4) confirmed this interaction. The proximity of the loop formed by Leu340 and Tyr341 forces the benzyl group to turn away from these side chains.

To verify this hypothesis, racemic *N*-benzylazaphosphinane derivatives were prepared as illustrated in Scheme 2. Ethyl divinylphosphinate **10** was obtained according to a previously reported procedure by addition of 2 equiv of vinyl magnesium bromide on ethyl dichlorophosphate **9**.[20] Addition of benzylamine at 100 °C for 16 h afforded the desired cyclic azaphosphinane **11** in good yield. The rest of the synthesis is carried out in the same way as described before, that is,

https://doi.org/10.1021/acs.jmedchem.0c02072
J. Med. Chem. 2021, 64, 3897−3910

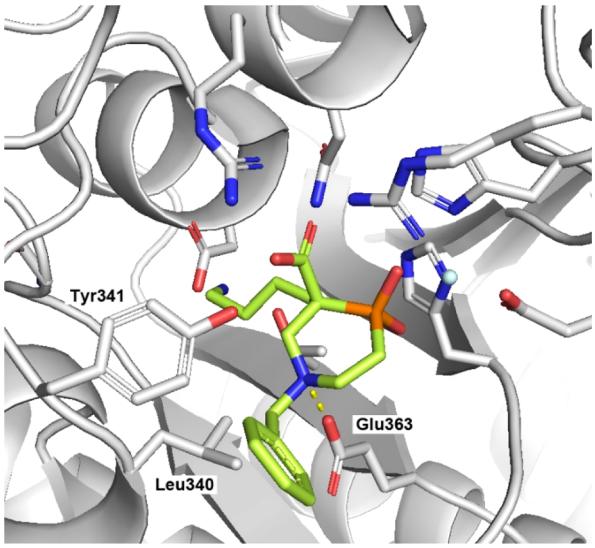

Figure 4. Docking of **14d** into TAFI (PDB 3D68) highlighting the interaction of the ring nitrogen with Glu363.

alkoxycarbonylation reaction followed by an alkylation reaction to introduce the basic side chain.

The resulting azaphosphinic acid ethyl ester **13a−c** was then quantitatively converted to the corresponding phosphinic acid with TMSBr followed by methanolysis. The final deprotection of the *t*-Bu ester was accomplished with 12 equiv of TFA in DCM to afford **14a−c**. The prepared cyclic azaphosphinane derivatives were also tested in the *in vitro* TAFIa inhibition assay and to our delight already the second compound synthesized (**14b**) showed remarkable activity with an IC_{50} = 186 nM as a racemic mixture (Table 2).

In comparison with **8e**, the introduction of the *N*-benzyl group into the cycle led to an impressive improvement of nearly 2 logs in potency. Variations in chain length confirmed the earlier findings that the optimal length is four carbons. The two enantiomers of **14b, 14d,** and **14e** were then isolated. As expected, only one of them was responsible for the inhibitory activity, **14d**. To assess its absolute configuration, crystallization attempts were carried out using a full-length TAFI with quintuple mutations in the dynamic flap next to the catalytic domain, named TAFI-CIIYQ: S327C, T347I, T351I, H355Y, and H357Q. Crystals of the TAFI-CIIYQ-**14d** complex were obtained by soaking and their X-ray structure confirmed the (*S*) configuration of the quaternary carbon center (Figure 5).

Although most of the 3D68-docked and the crystal structure of **14d** bound to TAFI were similar, one could observe a major difference in the binding site. The orientation of the benzyl group of **14d** was flipped between the two structures (Figure 5). Indeed, this benzyl group induced a pocket opening of the TAFI binding site. In PDB 3D68, the structure used for docking, the Tyr341 is turned toward the center of the active site, making a H-bond with the carboxylate of the ligand that is already making 2 H-bonds with Asn234 and Arg235. Due to the steric clash with the *N*-benzyl group of our molecules, the loop containing Leu340 and Tyr341 flips toward the outside of the pocket, and furthermore, the whole backbone of TAFI between Glu338 and Leu342 moves away, the largest displacement of 4.2 Å being observed for the C alpha of Leu340 (shown by a red arrow). This part of the backbone of TAFI was reported to be every flexible, as it is one end of the dynamic flap that can undergo large movements, leading to inactivation of TAFIa.[26] Tyr341 was not always visible as it rotates freely in the solvent. To assess the contribution of the ring nitrogen to the affinity, we synthesized the analogue of **14b** replacing the ring nitrogen atom by a carbon (**15**). This change led to some loss of potency with an IC_{50} = 0.5 μM for the most active racemic diastereoisomer **15** compared to 0.186 μM for those of **14b**.

Next, we evaluated the influence of the ring size. The corresponding 7-membered analogues were prepared according to Scheme 3. It is important to note that the unsubstituted azaphosphinane ring with 7 atoms is not symmetrical and two regio-isomers (**22** and **23**) are therefore produced after the carboxylation reaction with Boc-anhydride. Following separation by chromatography, these two compounds showed lower

Scheme 2. General Synthetic Route to *N*-Benzylazaphosphinane TAFIa Inhibitors 14a−c[a]

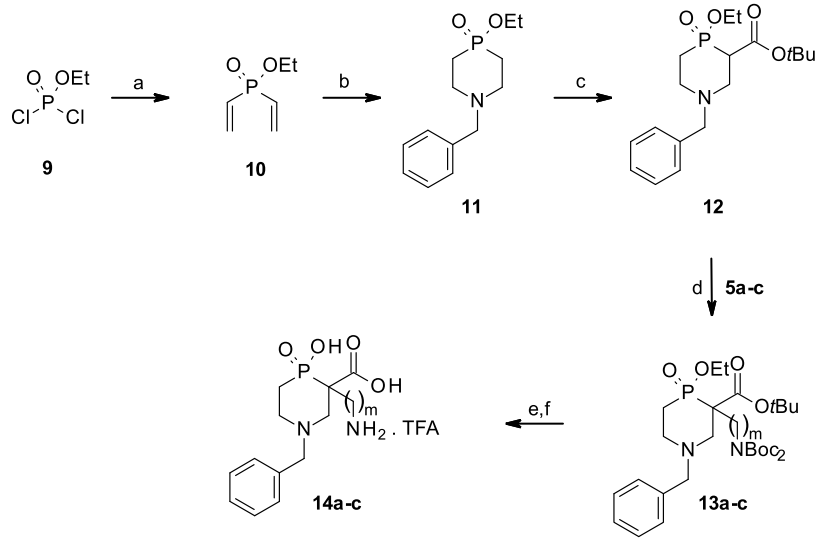

[a]Reagents and conditions: (a) vinyl magnesium bromide, THF, −78 °C, 2 h; (b) *N*-benzylamine, EtOH, reduced pressure, 100 °C, 16 h; (c) LDA, Boc_2O, THF, −70 °C, 2 h; (d) $Boc_2N-(CH_2)_n-Br$, NaH, DMSO, 10 °C; (e) TMS-Br, DCM, 0 °C, 20 h; (f) TFA, DCM, 20 °C, 10 h.

https://doi.org/10.1021/acs.jmedchem.0c02072
J. Med. Chem. 2021, 64, 3897−3910

Table 2. Inhibition of Human Activated TAFI by *N*-Benzylazaphosphinanes (14a–e, 15)

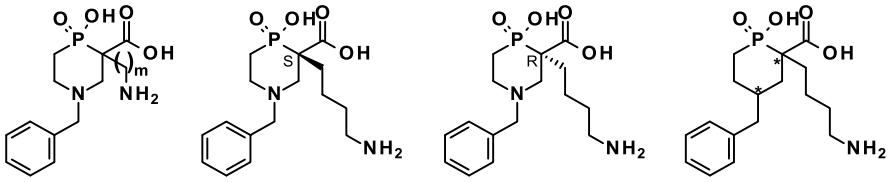

compounds	basic side chains	IC_{50} hTAFIa (μM)
14a	**5a**	>30.0
14b	**5b**	0.2
14c	**5c**	0.2
14d[a]	**5b**	0.1
14e[a]	**5b**	10.7
15[b]	**5b**	0.5

[a]**14d** and **14e** were isolated after chiral separation.[21] [b]**15** was synthesized starting from 2-(2-bromoethyl) but-3-enylbenzene according to the procedure described in the general synthetic scheme of cyclic phosphinane inhibitors and isolated as a mixture of 2 diastereoisomers (Scheme 1).

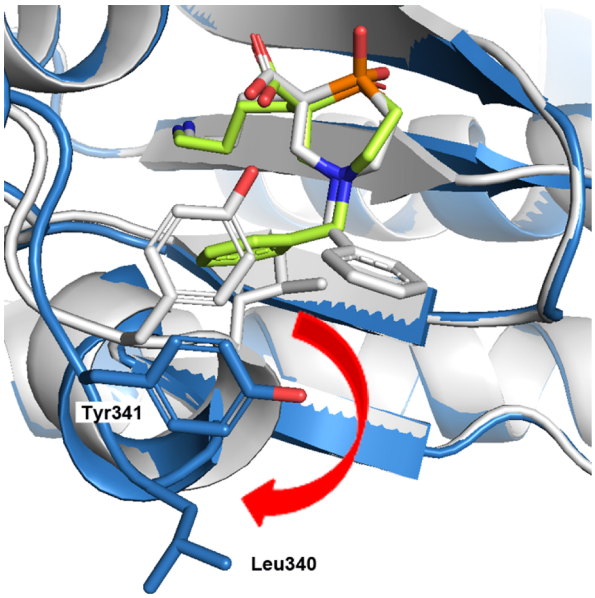

Figure 5. Docking (white) *vs* crystal (colored) structure of **14d** in complex with mutated TAFI. The red arrow shows the shift of Leu340 between 3D68 and the new X-ray structure (PDB code 7NEE).

activity compared to **14b** with IC_{50} of 1.9 and 0.6 μM, respectively.

Based on our observations so far, we concluded that if we would like to improve our TAFIa inhibitors, then we should explore the influence of the substitution on the nitrogen in the cycle. A new set of 6-membered azaphosphinane derivatives were designed, prioritized by docking, and synthesized according to the synthetic pathway shown in Scheme 4.

24 was obtained by hydrogenolysis of **13b** in the presence of Pd/C in ethanol and 1 equiv of HCl in 88% yield. The reductive amination of **24** was carried out in the presence of 1.5 equiv of aldehyde and anhydrous $MgSO_4$ followed by *in situ* reduction of the iminium intermediates by $NaBH(OAc)_3$ to afford **25a–n**. The simultaneous hydrolysis of the azaphosphinate ethyl ester and of the two Boc protecting groups was performed using TMS-Br followed by methanolysis of the intermediate silylated esters. Finally, 12 equiv of TFA were necessary to fully deprotect the *t*-Bu ester to lead to the targeted compounds **26a–l** as racemic mixtures of TFA salts.

The prepared compounds were tested in the *in vitro* TAFIa inhibition assay, and the results are summarized in Table 3. In the light of these results, replacement of the benzyl moiety by alkyl (**26b,c**) or cyclohexylmethyl (**26d**) was clearly detrimental. Elongation of the linker between the nitrogen and the benzene ring to 2 (**26e**) or 3 carbons (**26f**) led also to a significant drop of potency. A similar effect was observed when the phenyl group was replaced by heterocycles (**26g–l**), although the loss of potency was sometimes moderate, and the thiophen analogue **26l** that maintained activity against TAFIa (0.19 μM). In the pyridine series (**26g–i**), it appeared to us that only the 2-position was tolerated (**26i**).

Having identified that the benzyl substitution was optimal on the ring nitrogen, we evaluated the introduction of various substituents on the phenyl group in the hope of achieving a better occupation of the TAFIa catalytic site. Compounds **27a–n** were prepared following Scheme 4 and tested in the TAFIa inhibition assay (Table 4). Introducing a methoxy (**27a**) group in the para position led to a drop of efficacy due probably to a clash with the protein, while the hydroxy analogue **27b** showed a modest 2-fold improvement of the potency. Data obtained for the halogen-substituted analogue **27c–h** support the expectation based on the X-ray structure of **14d** that the substitution in the *o*- and *p*-position should be well tolerated. Replacement of the chlorine atom at the *o*-position by a bromine led to a more than 2-fold gain in potency (IC_{50} = 87 nM for **27h**), while change to fluorine resulted in a 3-fold drop underlining the importance of the size of the substituents at this position. In order to determine if in addition to its size, the nature of the substituents is also important, the corresponding biphenyl derivatives **27i–k** were also synthesized and tested. While the *m*- (**27j**) and *p*-biphenyls (**27k**) were inactive due probably to steric clash with the protein, **27i** achieved a vital 11-fold increase in potency compared to the simple benzyl derivative **14b** attaining an IC_{50} = 17 nM. The introduction of an oxygen between the two benzene rings (**27l**) killed the inhibitory effect, while replacement of the terminal benzene by a 3-pyridyl (**27m**) or 5-pyrimidyl (**27n**) ring gave very potent compounds with IC_{50}s of 2 and 7 nM, respectively.

The most advanced compounds tested so far were racemates, so in the final round of optimizations, we separated the two enantiomers by chiral chromatography and tested the more active ones **28a–k** (Table 4). In these compounds, we

https://doi.org/10.1021/acs.jmedchem.0c02072
J. Med. Chem. 2021, 64, 3897–3910

Scheme 3. General Synthetic Route to 7-Membered Ring Azaphosphinanes 22 and 23[a]

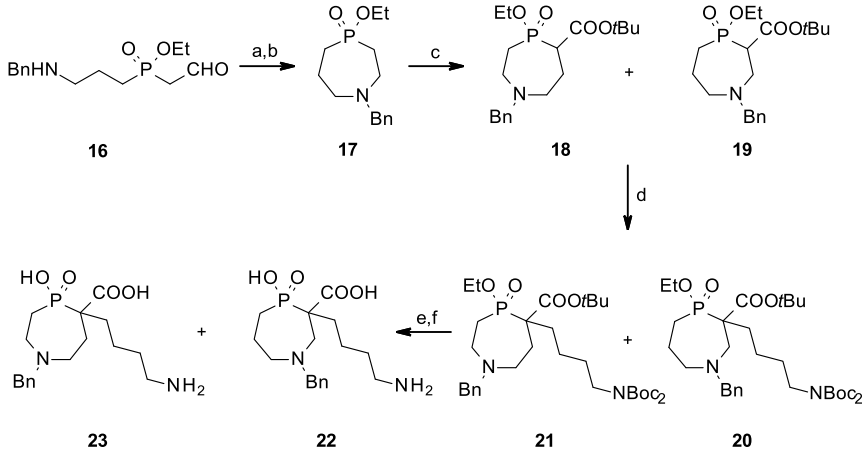

[a]Reagents and conditions: (a) $MgSO_4$, 20 °C, 1 h; (b) $NaBH(OAc)_3$, 20 °C, 16 h (c) LDA, Boc_2O, THF, −70 °C, 2 h; (d) $Boc_2N-(CH_2)_n-Br$, NaH, DMSO, 10 °C; (e) TMS-Br, DCM, 0 °C, 20 h; (f) TFA, DCM, 20 °C, 10 h.

Scheme 4. General Synthetic Route to N-Substituted Azaphosphinanes 26a−l and 27a−n[a]

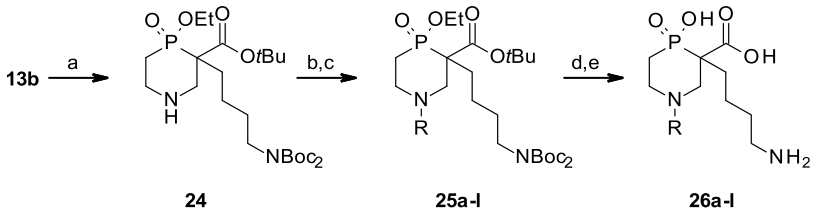

[a]Reagents and conditions: (a) 10% Pd/C (10 mol%), MeOH, 20 °C, 20 h (b) R−CHO, DCM, $MgSO_4$, 20 °C, 1 h; (c) $NaBH(OAc)_3$, 20 °C, 16 h; (d) TMS-Br, DCM, 0 °C, 20 h; (e) TFA, DCM, 20 °C, 10 h.

modified the benzene ring testing a variety of heterocycles with 5- or 6-membered rings, and we also modified the substituent in the *p*-position of the internal benzene ring in order to improve drug-like properties. Most of the prepared compounds showed very similar inhibitory activity around 10 nM. We managed to obtain the X-ray structure of **28k** complexed with TAFI (Figure 6).

Tyr341 is slightly rotated away from the active site making room for the pyrazole group. The backbone between Glu338 and Leu342 deviates from 3D68 and adopts a conformation more similar to that observed in the complex with **14d**. It is worth mentioning that the fluorine substituent on the benzene ring points directly at the backbone carbonyl oxygen of Ser299 at 4.1 Å explaining very moderate contribution to affinity from this interaction for the F- or HO-substituted analogues.

These cyclic azaphosphinanes have the distinction of being relatively polar compounds in general, with a clog $P < 1$ and a polar surface between 110 and 140 $Å^2$, which give them a very high aqueous solubility. As expected, these characteristics are responsible for the very low permeability and oral bioavailability as measured on the Caco-2 cell permeability assay. On the other hand, these compounds present very high metabolic stability when incubated with human or rat microsomes and hepatocytes (>70%) and a moderate to high unbound fraction in plasma (35−86%) as illustrated in Table 5 for **28k**. Finally, selectivity of compound **28k** was evaluated on human carboxypeptidases CPB (pancreatic) and CPN (plasmatic). **28k** is highly selective for TAFIa with a ratio of 7000 for CPB and more than 300,000 for CPN (Table 5).

A functional assay was set up to evaluate the ability of compounds showing an $IC_{50} \leq 20$ nM on human recombinant TAFIa to modulate the lysis of a blood clot. For that purpose, the lysis of rat blood clot was analyzed by thromboelastometry (TE), and activity of compounds was evaluated by their capacity to decrease the clot firmness (by AUC calculation), at the fixed dose of 0.8 μM or in a dose response for EC_{50} calculation (Table 6). Clotting time and clot formation time were not affected by any compounds (data not shown). Active compounds acted only on clot lysis acceleration and thus on clot firmness kinetics. The tested compounds at 0.8 μM dose showed decrease of lysis time in rat blood in the 43−79% range (Table 6). We determined the EC_{50} values for **28a** and **28k**, which were 378 and 389 nM, respectively. These EC_{50} values are significantly higher than the activity observed on human TAFIa (5 and 6 nM respectively, Table 4), suggesting a higher activity of these compounds on human TAFIa than in rat TAFIa, as described for mouse TAFIa.[22] The compounds showing *in vitro* inhibition over 40% were then tested for their duration of action in an *in vivo* pharmacodynamics model. Rats were treated by IV administration of vehicle or compounds at a 0.6 mg/kg dose and blood was collected 30 and 60 min later and percentage of inhibition of thromboelastogram AUC was evaluated at these 2 times (Table 6).

Most of the tested compounds showed a strong activity leading to an >50% decrease of AUC 30 min after IV administration, but the effect was usually not lasting, and activity decreased considerably 60 min after IV administration except for few products (**28g−k**). Analyzing the inhibitory activities, we can conclude that in general compounds having a

https://doi.org/10.1021/acs.jmedchem.0c02072
J. Med. Chem. 2021, 64, 3897−3910

Table 3. Inhibition of Human Activated TAFI by *N*-Benzylazaphosphinanes 26a−l

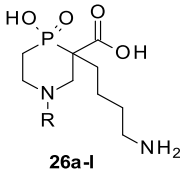

26a-l

Compounds	R	IC_{50} hTAFIa (μM)
26a	H	9.3
26b	Me	>30.0
26c	n-Pentyl	20.1
26d	Cyclohexylmethyl	>30.0
26e	Phenethyl	8.7
26f	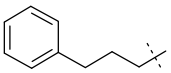	>30.0
26g	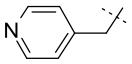	>30.0
26h	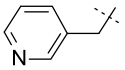	8.0
26i	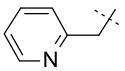	0.5
26j	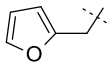	1.5
26k	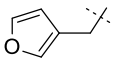	1.1
26l	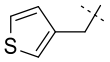	0.2

substituent in the "para" position of the benzene ring showed equal or better inhibitory activity after 60 min than their counterparts (c.f. **6a−6o**, **6m−6n**, **6p−6q**). The most efficient compound was **28k** with a remaining activity of 61% of lysis time decreasing 60 min after IV administration. Its activity and other properties supported its progression into preclinical and later clinical development. PK parameters in rat were determined for this compound (Table 5). Following single IV administration of **28k**, the terminal half-life was estimated to 0.47 h. The compound was eliminated with a low total clearance, almost entirely related to renal excretion. Moreover, **28k** is poorly distributed in tissues which has no impact as the targeted compartment is blood. In accordance with the low *in vitro* permeability (66%, Table 5), the *in vivo* oral bioavailability of **28k** was very low (F = 1%, 10 mg/kg *per os* in rat, C_{max} 98.7 ng/mL with a T_{max} at 45 min).

CONCLUSIONS

In conclusion, we have described here the discovery and the optimization of original, selective, and potent human TAFIa inhibitors. The SBDD led to the identification of **28k** that accelerates clot degradation and might increase vessel recanalization *in vivo*. Acceleration of endogenous fibrinolysis was confirmed *in vivo* in a murine model of pulmonary

Table 4. Inhibition of Human Activated TAFI by *N*-Benzylazaphosphinanes 27a−n and 28a−k

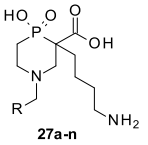

27a-n

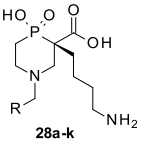

28a-k

Cpds	R	IC_{50} hTAFIa (nM) or %inh at 10 nM
27a	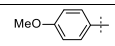	3104
27b	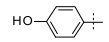	101
27c	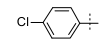	183
27d	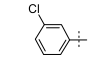	750
27e	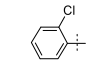	161
27f	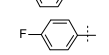	127
27g	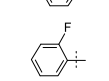	515
27h	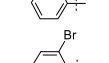	87
27i	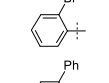	17
27j	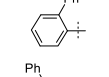	>30,000
27k	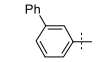	>30,000
27l	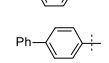	>30,000
27m	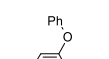	2
27n	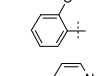	7
28a	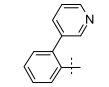	5
28b	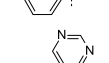	9
28c	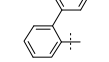	9
28d	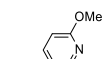	10
28e	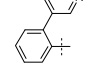	11
28f	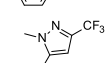	5
28g		10
28h	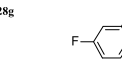	8
28i	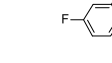	31
28j		8
28k	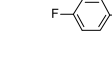	6
28l	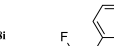	64% ± 1
28m	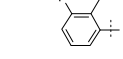	70% ± 7
28n		73% ± 5
28o	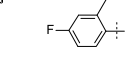	85% ± 3
28p		88% ± 1
28q		92% ± 9
28r		88% ± 12
28s		72% ± 6

https://doi.org/10.1021/acs.jmedchem.0c02072
J. Med. Chem. 2021, 64, 3897−3910

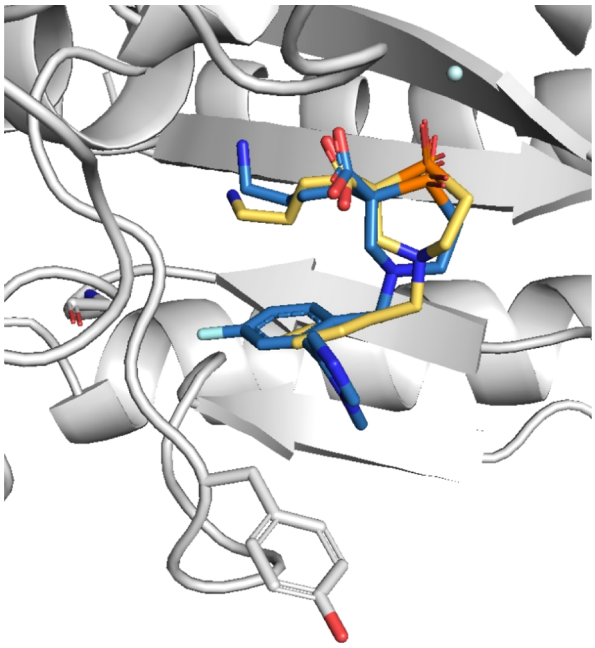

Figure 6. Overlay of the TAFI bound complexes of **28k** (blue, PDB code 7NEU) and **14d** (yellow, PDB code 7NEE).

Table 5. *In Vitro* ADME, Selectivity on CP and PK Parameters of 28k after Single IV Administration in Rat (1 mg/kg)

clog *P*	0.9
Fabs (ER)	66% (1.0)
plasma fu (m/r/hu)	93/89/95%
MFmic (r/m/hu)	100/100/100%
MFhep (r/m/hu)	100/100/85%
Ki (huTAFIa) μM	0.00075
Ki (huCPB) μM	5.3
Ki (huCPN) μM	282
AUC (μmol·h/L)	3.88
$t_{1/2}$, z (h)	0.47
CLp (mL/min/kg)	9.84
Vss (L/kg)	0.30
CLr (mL/min/kg)	9.54

thromboembolism after IV administration of **28k**.[22] Treatment with a TAFIa inhibitor, such as **28k** also known as **S62798**, could be a promising therapeutic option to treat patients with pulmonary embolism or ischemic stroke by accelerating blood vessel recanalization and improving patient outcome.

EXPERIMENTAL SECTION

General. All obtained products had a liquid chromatography purity above 96% that was corroborated by their ^{1}H NMR spectrum unless specifically mentioned otherwise. All synthetic experimental details including the characterization of the compounds are described in the Supporting Information. Examples **14d**, **14e**, **15**, **22**, and **23** have been prepared according to procedures already described.[21]

General Procedure B for the Preparation of Intermediates 13a−c. 60% NaH (8 mmol, 1.6 equiv) is added at 10 °C in portions to a solution of **5a−d** (5 mmol, 1 equiv) in DMSO (10 mL) under argon. Intermediate **12** (5 mmol) in solution in DMSO (5 mL) is then added to the suspension, and the mixture is stirred for 4 h at ambient temperature. The reaction mixture is then hydrolyzed with an aqueous NH_4Cl solution (50 mL) and extracted with EtOAc (2 × 100 mL). The organic phase is washed with H_2O (2 × 100 mL), dried over $MgSO_4$, and concentrated *in vacuo*. The residue obtained is purified by flash chromatography on silica gel using as eluant a DCM/EtOAc gradient (90:10 to 50:50). Intermediates **13a−c** are obtained as mixture of 4 diastereoisomers.

*tert-Butyl 3-{3-[bis(tert-Butoxycarbonyl)amino]propyl}-1-benzyl-4-ethoxy-4-oxo-1,4 Azaphosphinane-3-carboxylate (**13a**).* Intermediate **13a** is obtained starting from intermediates **12** and **5a** in accordance with procedure B described hereinbefore. White powder; yield 54% (0.225 g, 0.368 mmol). ^{1}H NMR (DMSO-d_6, 400 MHz): δ ppm 7.35−7.2 (m, 5H), 4 (m, 2H), 3.8 (m, 2H), centered at 3.52 (AB, 2H), 3−2.25 (m, 4H), 2−1.8 (m, 4H), 1.45−1.35 (2s, 27H), 1.2 (t, 3H), 1.2 (m, 2H).

*tert-Butyl 3-{4[bis(tert-Butoxycarbonyl)amino]butyl}-1-benzyl-4-ethoxy-4-oxo-1,4-azaphosphinane-3-carboxylate (**13b**).* Intermediate **13b** is obtained starting from intermediates **12** and **5b** in accordance with procedure B described hereinbefore. White powder; yield 79% (13.9 g, 22.248 mmol).^{1}H NMR (DMSO-d_6, 400 MHz): δ 7.30 (m, 5H), 3.97 (m, 2H), 3.63−3.43 (dd, 2H), 3.36 (m, 2H), 2.93−2.33 (m, 2H), 2.79−2.47 (m, 2H), 1.93 (m, 2H), 1.93 (m, 2H), 1.43 (m, 2H), 1.42 (s, 18H), 1.36 (s, 9H), 1.21 (t, 3H), 0.83 (m, 2H). IR (cm^{-1}): 1744, 1711 cm^{-1} (C═O), 1276 cm^{-1} (P═O).

*tert-Butyl 3-{5-bis(tert-Butoxycarbonyl)amino]pentyl}-1-benzyl-4-ethoxy-4-oxo-1,4-azaphosphinane-3-carboxylate (**13c**).* Intermediate **13c** is obtained starting from intermediates **12** and **5c** in accordance with procedure B described hereinbefore. White powder; yield 62% (0.310 g, 0.485 mmol). ^{1}H NMR (DMSO-d_6, 400 MHz): δ ppm 7.32−7.2 (m, 5H), 3.99 (m, 2H), 3.8 (m, 2H), centered at 3.5 (AB, 2H), 3−2.3 (m, 4H), 2−1.8 (m, 4H), 1.45−1.35 (2s, 27H), 1.35−1.15 (2m, 4H), 1.2 (t, 3H), 0.75 (m, 2H).

General Procedure C for the Synthesis of 14a−c. TMSBr (7.92 mL, 60 mmol, 12 equiv) is added dropwise to a solution of intermediate **13a−c** (5 mmol) in DCM (40 mL) under argon and at ambient temperature. The mixture is stirred for 16 h at ambient temperature and then concentrated *in vacuo*. The residue is taken up in MeOH (40 mL) and stirred for 20 min at ambient temperature, before being evaporated to dryness. The evaporate is dissolved in DCM (20 mL), and trifluoroacetic acid (44.6 mL, 60 mmol, 12 equiv) is added. The reaction mixture is stirred for 10 h at ambient temperature and then concentrated *in vacuo*. The residue obtained is purified by reverse-phase chromatography using as eluant an H_2O/MeCN gradient. The final racemic products **14a−c** (zwitterion) are isolated as a white solid after lyophilization.

*3-(3-Aminopropyl)-1-benzyl-4-hydroxy-4-oxo-1,4-azaphosphinane-3-carboxylic Acid (**14a**).* **14a** is obtained starting from

Table 6. Evaluation of the Activity *In Vitro* and *Ex Vivo* of Selected TAFIa Inhibitors by Thromboelastometry (TE) in Rat[a]

Cpds	TE *in vitro* % inhib ±SEM@0.8 μM (EC_{50} ± SEM in nM)	TE *ex vivo* % inhib@0.6 mg/kg 30/60 min post IV
28a	74% ± 3 (378 ± 56)	66/42
28c	66% ± 2	62/44
28f	43% ± 1	66/21
28g	63% ± 0	75/55
28h	71% ± 1	76/50
28k	57% ± 2 (389 ± 72)	NA/61
28l	61% ± 8	41/NA
28m	62% ± 2	60/13
28n	79% ± 2	78/30
28o	75% ± 6	NA/41
28p	67% ± 3	66/33
28q	68% ± 4	NA/45
28r	66% ± 3	63/19
28s	61% ± 4	80/17

[a]Percentage of inhibition (% inhib) represents the percentage of thromboelastogram AUC of the tested compound *vs* AUC of vehicle.

https://doi.org/10.1021/acs.jmedchem.0c02072
J. Med. Chem. 2021, 64, 3897−3910

intermediate **13a** in accordance with procedure C described hereinbefore. White powder; yield 56% (0.091 g, 0.279 mmol). ^{1}H NMR (D_2O, 400 MHz): δ ppm 7.5 (m, 5H), centred at 4.35 (AB, 2H), 3.75−3.35 (2m, 2H), 3.5−3.15 (2dd, 2H), 2.92 (t, 2H), 2.3−1.8 (2m, 2H), 1.95 (m, 1H), 1.6−1.4 (m, 3H). HRMS: calcd for [M + H] 327.1469; found, 327.1478. Elemental Anal. Calcd (%) for $C_{15}H_{23}N_2O_4P$: C, 55.21; H, 7.10; N, 8.58. Found: C, 55.38; H, 6.85; N, 8.58.

*3-(4-Aminobutyl)-1-benzyl-4-hydroxy-4-oxo-1,4-azaphosphinane-3-carboxylic Acid (**14b**).* **14b** is obtained in accordance with procedure C described hereinbefore starting from intermediate **13b**. White powder; yield 60% (1.628 g, 4.78 mmol).^{1}H NMR (DMSO-d_6, 400 MHz): δ ppm 8.2 (sl, 3H), 7.3 (m, 5H), 3.7−3.5 (2*(d, 1 + 1H), 3.05−2.4 (2*(m, 1 + 1H), 2.75−2.55 (2*(m, 1 + 1H), 2.7 (m, 2H), 1.8 (m, 1H), 1.6−1.1 (m, 7H). HRMS: calcd for $[M + H]^+$ 341.1626; found, 341.1628. Elemental Anal. Calcd (%) for $C_{16}H_{25}N_2O_4P$: C, 56.46; H, 7.40; N, 8.23. Found: C, 55.99; H, 7.14; N, 8.13.

*3-(5-Aminopentyl)-1-benzyl-4-hydroxy-4-oxo-1,4-azaphosphinane-3-carboxylic Acid (**14c**).* Example **14c** is obtained starting from intermediate **13c** in accordance with procedure C described hereinbefore. White powder; yield 51% (0.091g, 0.256 mmol). ^{1}H NMR (D_2O, 400 MHz): δ ppm 7.5 (m, 5H), centered at 4.32 (AB, 2H), 3.7−3.35 (2m, 2H), 3.5−3.1 (2dd, 2H), 2.9 (t, 2H), 2.2−1.78 (2m, 2H), 1.95−1.45 (2m, 2H), 1.6 (m, 2H), 1.3 (m, 2H), 1.1 (m, 2H). HRMS: calcdfor $[M + H]^+$ 355.1782; found, 355.1792. Elemental Anal. Calcd (%) for $C_{17}H_{27}N_2O_4P$: C, 57.62; H, 7.68; N, 7.90. Found: C, 58.04; H, 7.37; N, 7.95.

General Procedure D for the Synthesis of 26a−l, 27a−n. *tert-Butyl 3-{4-[bis(tert-Butoxycarbonyl)amino]butyl}-4-ethoxy-4-oxo-1,4-azaphosphinane-3-carboxylate (**24**).* Inter-mediate **13b** (73.6 g, 117.8 mmol), ethanol (1 L), Pd/C (7.36 g, 10% by mass), and 37% HCl (7.85 mL, 0.8 equiv) are introduced in succession into a 2 L flask at ambient temperature and under a stream of argon. The argon is then replaced by a hydrogen atmosphere. The reaction is monitored by LC/MS. After 4 h, the reaction is complete, and the catalyst is filtered off over a glass fiber. The filtrate is evaporated to dryness in order to obtain a yellow oil, which is taken up in EtOAc (400 mL) and in a 10% $NaHCO_3$ solution (400 mL). After decantation, the aqueous phase is extracted with EtOAc (3 × 100 mL). The organic phases are combined and then washed with a saturated NaCl solution (400 mL), dried over $MgSO_4$, and concentrated to yield the expected intermediate **24** as a white solid; yield 91% (57.6 g, 107.7 mmol). ^{1}H NMR (DMSO-d_6, 400 MHz): δ 9.8/8.6 (m, 2H), 4.2/4.0 (m, 2H), 3.5−3.2 (m, 6H), 2.4−1.8 (m, 4H), 1.55−1.3 (m, 2H), 1.45 (s, 18H), 1.40 (s, 9H), 1.28 (t, 3H), 1.5/0.9 (m, 4H). IR (KBr) (cm^{-1}): 3100−3500 cm^{-1} (OH), 3314 cm^{-1} (NH), 1712−1693 cm^{-1} (C═O).

The non-commercial aldehydes were prepared in accordance with the following procedure. Ethanol (500 mL), boronic acid Ar_2−$B(OH)_2$ (92.7 mmol, 1.2 equiv), and bromoarylaldehyde or bromoheteroarylaldehyde Br−Ar_1−CHO (77.3 mmol) are introduced in succession into a 1 L flask under argon and at ambient temperature. The solution is degassed with argon for 15 min. $Pd(PPh_3)_4$ (1.78 g, 1.55 mmol) and Na_2CO_3 (92.7 mL of a 2M solution in H_2O, 185 mmol, 2.4 equiv) are then introduced in a single portion. After the addition, the reaction mixture is heated at reflux for 5 h. The mixture is then evaporated to dryness. The residue is taken up in DCM (1 L) and H_2O (200 mL). After decantation, the aqueous phase is extracted with DCM (200 mL). The organic phases are combined and then washed with a saturated NaCl solution (400 mL), dried over $MgSO_4$ and concentrated under reduced pressure. The residue is then purified by flash chromatography on silica gel. The expected products are obtained in 59−94% yield.[21]

24 (14 g, 26.2 mmol), anhydrous DCM (280 mL), the desired aldehyde (39.3 mmol, 1.5 equiv), and $MgSO_4$ (14 g) are introduced in succession into a 500 mL three-necked flask at ambient temperature and under a stream of argon. After stirring for 1 h, $NaBH(OAc)_3$ (8.32 g, 39.3 mmol, 1.5 equiv) is added in portions, and the reaction mixture is maintained at ambient temperature for 16 h. The reaction is monitored by LC/MS. The insoluble components are filtered off over a microfiber and rinsed with DCM (100 mL). The filtrate is then washed with water (1 × 200 mL) and then with a saturated NaCl solution (2 × 200 mL). The organic phase is dried over $MgSO_4$ and concentrated under reduced pressure. The oil obtained is then purified by flash chromatography on silica gel (330 g) to yield intermediates **25**.

Examples **26** and **27** are obtained starting from intermediates **25** in accordance with the procedure C described hereinbefore. The yields given are for the last 2 steps from their corresponding intermediates **25a−n**.

*3-(4-Aminobutyl)-4-hydroxy-4-oxo-1,4-azaphosphinane-3-carboxylic Acid (**26a**).* White solid; yield 48% (0.108 g, 0.431 mmol). ^{1}H NMR (D_2O, 400 MHZ): δ ppm 3.5−3.65 (2m, 2H), 3.2 (m, 1H), 3.05 (dd, 1H), 2.95 (m, 2H), 2.15 (m, 1H), 1.95 (m, 1H), 1.75 (m, 1H), 1.65 (m, 2H), 1.5 (m, 1H), 1.4 (m, 1H), 1.25 (m, 1H). HRMS: calcd for $[M + H]^+$ 251.1156; found: 251.1154. Elemental Anal. Calcd (%) for $C_9H_{19}N_2O_4P$: C, 43.20; H, 7.65; N, 11.20. Found: C, 42.65; H, 7.23; N, 11.24.

*3-(4-Aminobutyl)-4-hydroxy-1-methyl-4-oxo-1,4-azaphosphinane-3-carboxylic Acid (**26b**).* White solid; yield 65% (0.150 g, 0.567 mmol).^{1}H NMR (D_2O, 400 MHZ): δ ppm 3.7−3.5 (m, 2H), 3.3 (t, 1H), 3.2 (dd, 1H), 3 (t, 2H), 2.9 (s, 3H), 2.3 (m, 1H), 2 (m, 1H), 1.75 (m, 1H), 1.7 (m, 2H), 1.5 (m, 1H), 1.4−1.25 (2m, 2H). HRMS: calcd for $[M + H]^+$ 265.1313; found, 265.1300. Elemental Anal. Calcd (%) for $C_{10}H_{21}N_2O_4P$: C, 45.45; H, 8.01; N, 10.60. Found: C, 45.59; H, 7.97; N, 10.61.

*3-(4-Aminobutyl)-4-hydroxy-4-oxo-1-pentyl-1,4-azaphosphinane-3-carboxylic Acid (**26c**).* White solid; yield 59% (0.141 g, 0.44 mmol). ^{1}H NMR (D_2O, 400 MHZ): δ ppm 3.7−3.5 (m, 2H), 3.3 (m, 1H), 3.15−3 (2m, 5H), 2.27 (m, 1H), 2 (m, 1H), 1.85−1.6 (m, 5H), 1.5−1.41 (2m, 2H), 1.3 (m, 5H), 0.85 (t, 3H). HRMS: calcd for [M + H]$^+$ 321.1939; found, 321.1933. Elemental Anal. Calcd (%) for $C_{14}H_{29}N_2O_4P$: C, 52.49; H, 9.12; N, 8.74. Found: C, 52.77; H, 8.93; N, 9.00.

*3-(4-Aminobutyl)-1-(cyclohexylmethyl)-4-hydroxy-4-oxo-1,4-azaphosphinane-3-carboxylic Acid (**26d**).* White solid; yield 62% (0.167 g, 0.482 mmol). ^{1}H NMR (D_2O, 400 MHZ): δ ppm 3.7−3.25 (2m, 2H), 3.55−3.15 (2dd, 2H), 3.1−2.9 (t + 2dd, 4H), 2.25 (m, 1H), 2 (m, 1H), 1.85−1.55 (m, 9H), 1.52−1.41 (2m, 2H), 1.3−1.1 (m, 4H), 1 (m, 2H). HRMS: calcd for [M + H]$^+$ 347.2095; found, 347.2095. Elemental Anal. Calcd (%) for $C_{16}H_{31}N_2O_4P$: C, 55.48; H, 9.02; N, 8.09. Found: C, 55.29; H, 9.08; N, 7.95.

*3-(4-Aminobutyl)-4-hydroxy-4-oxo-1-(2-phenylethyl)-1,4-azaphosphinane-3-carboxylic Acid (**26e**).* White solid; yield 40% (0.124 g, 0.35 mmol). ^{1}H NMR (D_2O, 400 MHZ): δ ppm 7.4−7.25 (m, 5H), 3.7−3.3 (2m, 2H), 3.52 (m, 1H), 3.45 (t, 2H), 3.1 (m, 3H), 2.95 (m, 2H), 2.2−1.75 (2m, 2H), 1.95 (m, 1H), 1.62 (m, 2H), 1.5−1.1 (m, 3H). HRMS: calcd for $[M + H]^+$ 355.1782; found, 355.1777. Elemental Anal. Calcd (%) for $C_{17}H_{27}N_2O_4P$: C, 57.62; H, 7.68; N, 7.90. Found: C, 57.63; H, 7.36; N, 7.90.

*3-(4-Aminobutyl)-4-hydroxy-4-oxo-1-(3-phenylpropyl)-1,4-azaphosphinane-3-carboxylic Acid (**26f**).* White solid; yield 66% (0.204 g, 0.554 mmol). ^{1}H NMR (D_2O, 400 MHZ): δ ppm 7.38 (t, 2H), 7.27 (m, 3H), 3.62−3.28 (2m, 2H), 3.52 (dd, 1H), 3.11 (m, 3H), 3 (td, 2H), 2.7 (t, 2H), 2.25−1.75 (2m, 2H), 2.09 (m, 2H), 1.95−1.5 (2m, 2H), 1.65 (m, 2H), 1.38−1.22 (2m, 2H). HRMS: calcd for [M + H]$^+$ 369.1939; found, 369.1950. Elemental Anal. Calcd (%) for $C_{18}H_{29}N_2O_4P$: C, 58.68; H, 7.93; N, 7.60. Found: C, 58.68; H, 7.45; N, 7.54.

*3-(4-Aminobutyl)-4-hydroxy-4-oxo-1-(pyridin-4-ylmethyl)-1,4-azaphosphinane-3-carboxylic Acid (**26g**).* White solid; yield 41% (0.09 g, 0.267 mmol). ^{1}H NMR (DMSO-d_6, 400 MHZ): δ ppm 8.5 (d, 2H), 8.05 (m, 3H), 7.3 (d, 2H), 3.55 (AB, 2H), 3.05−2.3 (2m, 2H), 2.7 (m, 3H), 2.5 (m, 1H), 1.75 (m, 1H), 1.65−1.15 (m, 7H). HRMS: calcd for $[M + H]^+$ 342.1578; found, 342.1577. Elemental Anal. Calcd (%) for $C_{15}H_{24}N_3O_4P$: C, 52.78; H, 7.09; N, 12.31. Found: C, 52.56; H, 6.70; N, 12.22.

*3-(4-Aminobutyl)-4-hydroxy-4-oxo-1-(pyridin-3-ylmethyl)-1,4-azaphosphinane-3-carboxylic Acid (**26h**).* White solid; yield 58% (0.140 g, 0.41 mmol). ^{1}H NMR (D_2O, 400 MHZ): δ ppm 8.6 (s + d, 2H), 8 (dd, 1H), 7.52 (dd, 1H), 4.4 (AB, 2H), 3.7 (m, 1H), 3.4 (m,

https://doi.org/10.1021/acs.jmedchem.0c02072
J. Med. Chem. 2021, 64, 3897−3910

2H), 3.18 (dd, 1H), 2.9 (m, 2H), 2.28−1.8 (2m, 2H), 1.91 (m, 1H), 1.6 (m, 2H), 1.5 (m, 1H), 1.21−1.1 (2m, 2H). HRMS: calcd for $[M + H]^+$ 342.1578; found, 342.1568. Elemental Anal. Calcd (%) for $C_{15}H_{24}N_3O_4P$: C, 52.78; H, 7.09; N, 12.31. Found: C, 52.32; H, 6.66; N, 12.32.

*3-(4-Aminobutyl)-4-hydroxy-4-oxo-1-(pyridin-2-ylmethyl)-1,4-azaphosphinane-3-carboxylic Acid (**26i**).* White solid; yield 57% (0.140 g, 0.41 mmol). ^{1}H NMR (D_2O, 400 MHZ): δ ppm 8.6 (dd, 1H), 7.91 (t, 1H), 7.55 (d, 1H), 7.45 (dd, 1H), centered at 4.41 (AB, 2H), 3.75−3.4 (2m, 2H), 3.55−3.3 (2dd, 2H), 2.95 (m, 2H), 2.3−1.78 (2m, 2H), 1.98 (m, 1H), 1.65 (m, 2H), 1.5 (m, 1H), 1.3−1.2 (2m, 2H). HRMS: calcd for $[M + H]^+$ 342.1578; found, 342.1562. Elemental Anal. Calcd (%) for $C_{15}H_{24}N_3O_4P$: C, 52.78; H, 7.09; N, 12.31. Found: C, 52.72; H, 6.92; N, 12.25.

*3-(4-Aminobutyl)-1-(furan-2-ylmethyl)-4-hydroxy-4-oxo-1,4-azaphosphinane-3-carboxylic Acid (**26j**).* White solid; yield 57% (0.12 g, 0.363 mmol). ^{1}H NMR (D_2O, 400 MHZ): δ ppm 7.6 (sl, 1H), 6.7 (tf, 1H), 6.5 (tf, 1H), 4.45−4.32 (2d, 2H), 3.7−3.3 (2m, 2H), 3.52−3.12 (2m, 2H), 2.98 (m, 2H), 2.25−1.8 (2m, 2H), 1.95−1.5 (2m, 2H), 1.62 (m, 2H), 1.32−1.2 (2m, 2H). HRMS: calcd for $[M + H]^+$ 331.1419; found, 331.1422. Elemental Anal. Calcd (%) for $C_{14}H_{23}N_2O_5P$: C, 50.91; H, 7.02; N, 8.48. Found: C, 50.48; H, 6.48; N, 8.37.

*3-(4-Aminobutyl)-1-(furan-3-ylmethyl)-4-hydroxy-4-oxo-1,4-azaphosphinane-3-carboxylic Acid (**26k**).* White solid; yield 38% (0.105 g, 0.318 mmol). ^{1}H NMR (D_2O, 400 MHZ): δ ppm 7.71 (sl, 1H), 7.59 (sl, 1H), 6.58 (sl, 1H), 4.22 (m, 2H), 3.7−3.35 (2m, 2H), 3.55−3.08 (2dd, 2H), 2.95 (m, 2H), 2.25−1.8 (2m, 2H), 1.95−1.5 (2m, 2H), 1.62 (m, 2H), 1.31−1.18 (2m, 2H). HRMS: calcd for $[M + H]^+$ 331.1419; found, 331.1431. Elemental Anal. Calcd (%) for $C_{14}H_{23}N_2O_5P$: C, 50.91; H, 7.02; N, 8.48. Found: C, 50.45; H, 6.72; N, 8.39.

*3-(4-Aminobutyl)-4-hydroxy-4-oxo-1-(thiophen-3-ylmethyl)-1,4-azaphosphinane-3-carboxylic Acid (**26l**).* White solid; yield 31 % (0.201 g, 0.58 mmol). ^{1}H NMR (D_2O, 400 MHZ): δ ppm 7.61 (d, 1H), 7.54 (dd, 1H), 7.2 (d, 1H), 4.42−4.28 (2*d, 2H), 3.71−3.32 (m, 2H), 3.48−3.06 (m, 2H), 2.94 (m, 2H), 2.25−1.77 (m, 2H), 1.93−1.46 (m, 2H), 1.6 (m, 2H), 1.26−1.13 (m, 2H). HRMS: calcd for $[M + H]^+$ 347.1190; found, 347.1182. Elemental Anal. Calcd (%) for $C_{14}H_{23}N_2O_4PS$: C, 48.55; H, 6.69; N, 8.09; S, 9.26. Found: C, 48.55; H, 6.55; N, 7.87; S, 8.65.

*3-(4-Aminobutyl)-4-hydroxy-1-[(4-methoxyphenyl)methyl]-4-oxo-1,4-azaphosphinane-3-carboxylic Acid (**27a**).* White solid; yield 59% (0.180 g, 0.486 mmol). ^{1}H NMR (D_2O, 400 MHZ): δ ppm 7.41 (d, 2H), 7.02 (d, 2H), 4.25 (m, 2H), 3.8 (s, 3H), 3.7−3.3 (2m, 2H), 3.45−3.08 (2dd, 2H), 2.95 (m, 2H), 2.25−1.75 (2m, 2H), 1.95−1.45 (2m, 2H), 1.6 (m, 2H), 1.25−1.1 (2m, 2H). HRMS: calcd for $[M + H]^+$ 371.1732; found, 371.1719. Elemental Anal. Calcd (%) for $C_{17}H_{27}N_2O_5P$: C, 55.13; H, 7.35; N, 7.56. Found: C, 54.93; H, 7.41; N, 7.56.

*3-(4-Aminobutyl)-4-hydroxy-1-[(4-hydroxyphenyl)methyl]-4-oxo-1,4-azaphosphinane-3-carboxylic Acid (**27b**).* White solid; yield 56% (0.135 g, 0.379 mmol). ^{1}H NMR (D_2O, 400 MHZ): δ ppm 7.38 (d, 2H), 6.95 (d, 2H), 4.25 (m, 2H), 3.7−3.3 (2m, 2H), 3.48−3.05 (2dd, 2H), 2.95 (m, 2H), 2.21−1.75 (2m, 2H), 1.95−1.5 (2m, 2H), 1.6 (m, 2H), 1.25−1.11 (2m, 2H). HRMS: calcd for $[M + H]^+$ 371.1732; found, 371.1712. Elemental Anal. Calcd (%) for $C_{16}H_{25}N_2O_5P$: C, 53.93; H, 7.07; N, 7.86. Found: C, 53.24; H, 6.89; N, 7.57.

*3-(4-Aminobutyl)-1-[(4-chlorophenyl)methyl]-4-hydroxy-4-oxo-1,4-azaphosphinane-3-carboxylic Acid (**27c**).* White solid; yield 68% (0.205 g, 0.545 mmol). ^{1}H NMR (D_2O, 400 MHZ): δ ppm 7.5−7.45 (2d, 4H), 4.41−4.21 (2d, 2H), 3.7−3.33 (2m, 2H), 3.45−3.1 (2dd, 2H), 2.95 (m, 2H), 2.25−1.78 (2m, 2H), 1.95−1.5 (2m, 2H), 1.6 (m, 2H), 1.25−1.1 (2m, 2H). HRMS: calcd for $[M + H]^+$ 375.1236; found, 375.1242. Elemental Anal. Calcd (%) for $C_{16}H_{24}ClN_2O_4P$: C, 51.27; H, 6.45; N, 7.47. Found: C, 50.89; H, 6.01; N, 7.44.

*3-(4-Aminobutyl)-1-[(3-chlorophenyl)methyl]-4-hydroxy-4-oxo-1,4-azaphosphinane-3-carboxylic Acid (**27d**).* White solid; yield 43% (0.123 g, 0.328 mmol). ^{1}H NMR (D_2O, 400 MHZ): δ ppm 7.52−7.35 (m, 4H), 4.32 (m, 2H), 3.7−3.32 (2m, 2H), 3.5−3.12 (2dd, H), 2.93 (m, 2H), 2.25−1.8 (2m, 2H), 1.95−1.48 (2m, 2H), 1.6 (m, 2H), 1.25−1.11 (2m, 2H). HRMS: calcd for $[M + H]^+$ 375.1236; found, 375.1256. Elemental Anal. Calcd (%) for $C_{16}H_{24}ClN_2O_4P$: C, 51.27; H, 6.45; N, 7.47. Found: C, 51.26; H, 6.32; N, 7.43.

*3-(4-Aminobutyl)-1-[(2-chlorophenyl)methyl]-4-hydroxy-4-oxo-1,4-azaphosphinane-3-carboxylic Acid (**27e**).* White solid; yield 64% (0.224 g, 0.598 mmol). ^{1}H NMR (D_2O, 400 MHZ): δ ppm 7.58−7.53 (2d, 2H), 7.48−7.4 (2m, 2H), 4.44 (m, 2H), 3.71−3.41 (2m, 2H), 3.51−3.28 (2m, 2H), 2.94 (m, 2H), 2.22−1.78 (2m, 2H), 1.95−1.61 (2m, 2H), 1.6−1.49 (2m, 2H), 1.28−1.11 (2m, 2H). ^{31}P NMR: (D2O, 400 MHZ): δ ppm −25.5. HRMS: calcd for $[M + H]^+$ 375.1236; found, 375.1235. Elemental Anal. Calcd (%) for $C_{16}H_{24}ClN_2O_4P$: C, 51.27; H, 6.45; N, 7.47. Found: C, 51.58; H, 6.22; N, 7.65.

*3-(4-Aminobutyl)-1-[(4-fluorophenyl)methyl]-4-hydroxy-4-oxo-1,4-azaphosphinane-3-carboxylic Acid (**27f**).* White solid; yield 72% (0.21 g, 0.586 mmol). ^{1}H NMR (D_2O, 400 MHZ): δ ppm 7.5 (dd, 2H), 7.2 (t, 2H), 4.41−4.21 (2d, 2H), 3.7−3.31 (2m, 2H), 3.45−3.1 (2dd, 2H), 2.95 (m, 2H), 2.25−1.78 (2m, 2H), 1.95−1.5 (2m, 2H), 1.6 (m, 2H), 1.25−1.1 (2m, 2H). HRMS: calcd for $[M + H]^+$ 359.1532; found, 359.1532. Elemental Anal. Calcd (%) for $C_{16}H_{24}FN_2O_4P$: C, 53.65; H, 6.75; N, 7.82. Found: C, 53.65; H, 6.20; N, 7.83.

*3-(4-Aminobutyl)-1-[(2-fluorophenyl)methyl]-4-hydroxy-4-oxo-1,4-azaphosphinane-3-carboxylic Acid (**27g**).* White solid; yield 73% (0.243 g, 0.678 mmol).^{1}H NMR (D_2O, 300 MHZ): δ ppm 7.5 (m, 2H), 7.26 (m, 2H), 4.41 (sl, 2H), 3.7−3.35 (2m, 2H), 3.52−3.21 (2m, 2H), 2.94 (m, 2H), 2.22−1.77 (2m, 2H), 1.95−1.49 (2m, 2H), 1.61 (quint., 2H), 1.28−1.14 (2m, 2H). ^{19}F NMR: (D_2O, 300 MHZ): δ ppm −115. ^{31}P NMR: (D_2O, 300 MHZ): δ ppm 25.6. HRMS: calcd for $[M + H]^+$ 359.1532; found, 359.1530. Elemental Anal. Calcd (%) for $C_{16}H_{24}FN_2O_4P$: C, 53.65; H, 6.75; N, 7.82. Found: C, 53.34; H, 6.46; N, 7.77.

*3-(4-Aminobutyl)-1-[(2-bromophenyl)methyl]-4-hydroxy-4-oxo-1,4-azaphosphinane-3-carboxylic Acid (**27h**).* White solid; yield 48% (0.188 g, 0.449 mmol). ^{1}H NMR (D_2O, 300 MHZ): δ ppm 7.75 (dl, 1H), 7.53 (dd, 1H), 7.45 (tl, 1H), 7.39 (td, 1H), 4.44 (AB, 2H), 3.74−3.43 (2m, 2H), 3.5−3.28 (2m, 2H), 2.94 (m, 2H), 2.24−1.79 (2m, 2H), 1.95−1.5 (2m, 2H), 1.6 (m, 2H), 1.26−1.1 (2m, 2H). HRMS: calcd for $[M + H]^+$ 419.0731; found, 419.0732. Elemental Anal. Calcd (%) for $C_{16}H_{24}BrN_2O_4P$: C, 45.84; H, 5.77; N, 6.68. Found: C, 45.33; H, 5.29; N, 7.00.

*3-(4-Aminobutyl)-4-hydroxy-4-oxo-1-[(2-phenylphenyl)-methyl]-1,4-azaphosphinane-3-carboxylic Acid (**27i**).* White solid; yield 70% (0.274 g, 0.658 mmol).^{1}H NMR (DMSO-d_6, 400 MHZ): δ ppm 7.65−7.3 (m, 6H), 4.33 (AB, 2H), 3.43−3 (m, 3H), 2.92 (dd, 1H), 2.82 (m, 2H), 2.06−1.57 (2m, 2H), 1.83−1.33 (2m, 2H), 1.57 (m, 2H), 1.08 (m, 2H). HRMS: calcd for $[M + H]^+$ 417.1939; found, 417.1945. Elemental Anal. Calcd (%) for $C_{22}H_{29}N_2O_4P$: C, 63.68; H, 7.02; N, 6.73. Found: C, 63.68; H, 6.84; N, 6.85.

*3-(4-Aminobutyl)-4-hydroxy-4-oxo-1-[(3-phenylphenyl)methyl]-1,4-azaphosphinane-3-carboxylic Acid (**27j**).* White solid; yield 40% (0.157 g, 0.377 mmol). H NMR (D_2O, 400 MHZ): δ ppm 7.79−7.4 (m, 9H), 4.49 (m, 1H), 4.29 (d, 1H), 3.76 (m, 1H), 3.51 (dd, 1H), 3.39 (m, 1H), 3.13 (dd, 1H), 2.89 (m, 2H), 2.27 (m, 1H), 1.92 (m, 1H), 1.79 (m, 1H), 1.58 (m, 2H), 1.48 (m, 1H), 1.21 (m, 1H), 1.09 (m, 1H). HRMS: calcd for $[M + H]^+$ 417.1939; found, 417.1937. Elemental Anal. Calcd (%) for $C_{22}H_{29}N_2O_4P$: C, 63.68; H, 7.02; N, 6.73. Found: C, 63.45; H, 6.72; N, 6.86.

*3-(4-Aminobutyl)-4-hydroxy-4-oxo-1-[(4-phenylphenyl)-methyl]-1,4-azaphosphinane-3-carboxylic Acid (**27k**).* White solid; yield 50% (0.175 g, 0.42 mmol). ^{1}H NMR (D_2O, 400 MHZ): δ ppm 7.8 (d, 2H), 7.7 (d, 2H), 7.55 (d, 2H), 7.5 (t, 2H), 7.41 (t, 1H), 4.45−4.28 (2d, 2H), 3.75−3.35 (2m, 2H), 3.5−3.15 (2dd, 2H), 2.9 (m, 2H), 2.25−1.8 (2m, 2H), 1.95−1.45 (2m, 2H), 1.6 (m, 2H), 1.25−1.1 (2m, 2H). HRMS: calcd for $[M + H]^+$ 417.1939; found, 417.1932. Elemental Anal. Calcd (%) for $C_{22}H_{29}N_2O_4P$: C, 63.68; H, 7.02; N, 6.73. Found: C, 63.25; H, 6.64; N, 6.55.

https://doi.org/10.1021/acs.jmedchem.0c02072
J. Med. Chem. 2021, 64, 3897−3910

*3-(4-Aminobutyl)-4-hydroxy-4-oxo-1-[(2-phenoxyphenyl)-methyl]-1,4-azaphosphinane-3-carboxylic Acid (**27l**).* White solid; yield 61% (0.249 g, 0.515 mmol). ^{1}H NMR (D_2O, 300 MHZ): δ ppm 7.47 (t, 1H), 7.41 (t, 2H), 7.27−7.09 (m, 4H), 7.05 (d, 2H), 4.27 (m, 2H), 3.68−3.3 (2m, 2H), 3.46−3.07 (2m, 2H), 2.91 (m, 2H), 2.23−1.76 (2m, 2H), 1.93−1.46 (2m, 2H), 1.6 (quint., 2H), 1.15 (m, 2H). ^{31}P NMR: (D_2O, 300 MHZ): δ ppm 25.8. HRMS: calcd for $[M + H]^+$ 433.1888; found, 433.1894. Elemental Anal. Calcd (%) for $C_{22}H_{29}N_2O_5P$: C, 61.51; H, 6.76; N, 6.48. Found: C, 61.51; H, 6.57; N, 6.67.

*3-(4-Aminobutyl)-4-hydroxy-4-oxo-1-[(2-pyridin-3-ylphenyl)-methyl]-1,4-azaphosphinane-3-carboxylic Acid (**27m**).* White solid; yield 67% (0.2 g, 0.479 mmol). ^{1}H NMR (D_2O, 400 MHZ): δ ppm 8.58 (dd, 1H), 8.51 (d, 1H), 7.86 (dt, 1H), 7.67 (m, 1H), 7.58 (m, 1H), 7.58 (m, 2H), 7.43 (m, 1H), 4.42−4.3 (2*d, 2H), 3.46−3.11 (m, 2H), 3.2−2.87 (m, 2H), 2.94 (m, 2H), 2.11−1.65 (m, 2H), 1.86−1.36 (m, 2H), 1.59 (m, 2H), 1.08 (m, 2H). MS HRMS: calcd for $[M + H]^+$ 418.1891; found, 418.1898. Elemental Anal. Calcd (%) for $C_{21}H_{28}N_3O_4P$: C, 60.42; H, 6.76; N, 10.07; Found: C, 60.58; H, 6.51; N, 10.09.

*3-(4-Aminobutyl)-4-hydroxy-4-oxo-1-[(2-pyrimidin-5-ylphenyl)-methyl]-1,4-azaphosphinane-3-carboxylic Acid (**27n**).* White solid; yield 67% (0.187 g, 0.447 mmol). ^{1}H NMR (D_2O, 400 MHZ): δ ppm 9.19 (s, 1H), 8.85 (s, 2H), 7.7 (m, 1H), 7.68−7.59 (m, 2H), 7.45 (m, 1H), 4.38 (dd, 2H), 3.52−3.15 (2m, 2H), 3.25−2.9 (2m, 2H), 2.9 (m, 2H), 2.1−1.7 (2m, 2H), 1.85−1.4 (2m, 2H), 1.6 (m, 2H), 1.1 (m, 2H). HRMS: calcd for $[M + H]^+$ 419.1844; found, 419.1856. Elemental Anal. Calcd (%) for $C_{20}H_{27}N_4O_4P$: C, 57.41; H, 6.50; N, 13.39. Found: C, 57.94; H, 6.37; N, 13.40.

General Procedure E for the Synthesis of 28a−s. Examples **28a−s** are obtained starting from (***S***)-**24** in accordance with the procedure D described hereinbefore. The yields given are for the last 2 steps of their synthesis that is from their corresponding enantiopure intermediates (***S***)-**25a−s**.

*(3S)-3-(4-Aminobutyl)-4-hydroxy-1-[2-(6-methoxypyridin-3-yl)-benzyl]-4-oxo-1,4-azaphosphinane-3-carboxylic Acid (**28a**).* White solid; yield 91% (6.11 g, 13.654 mmol). ^{1}H NMR (D_2O, 400 MHZ): δ ppm 8.05 (d, 1H), 7.75 (dd, 1H), 7.6 (m, 1H), 7.5 (m, 2H), 7.4 (m, 1H), 7 (d, 1H), 4.3 (dd, 2H), 3.9 (s, 3H), 3.45−3.15 (2m, 2H), 3.2−2.85 (2dd, 2H), 2.9 (m, 2H), 2.1−1.7 (2m, 2H), 1.8−1.35 (2m, 2H), 1.6 (m, 2H), 1.1 (m, 2H). HRMS: calcd for $[M + H]^+$ 448.1997; found, 448.2006. Elemental Anal. Calcd (%) for $C_{22}H_{30}N_3O_5P$: C, 59.05; H, 6.76; N, 9.39. Found: C, 58.81; H, 6.79; N, 9.31. RP: −11.510 (589 nm, T = 19 °C, C = 0.9).

*(3S)-3-(4-Aminobutyl)-4-hydroxy-1-[[2-[2-methyl-5-(trifluoromethyl)pyrazol-3-yl]phenyl]methyl]-4-oxo-1,4-azaphosphinane-3-carboxylic Acid (**28b**).* White solid; yield 90% (1.304 g, 2.67 mmol). ^{1}H NMR (D_2O, 300 MHZ): δ ppm 7.63−7.46 (m, 4H), 6.81 (s, 1H), 4.21 (m, 2H), 3.65 (s, 3H), 3.5−3.19 (2m, 2H), 3.26−3 (2m, 2H), 2.91 (m, 2H), 2.15−1.69 (2m, 2H), 1.87−1.4 (2m, 2H), 1.58 (m, 2H), 1.11 (m, 2H) | NMR ^{19}F (D_2O, 300 MHZ): δ ppm −61.8. HRMS: calcd for $[M + H]^+$ 489.1874; found, 489.1903. Elemental Anal. Calcd (%) for $C_{21}H_{28}F_3N_4O_4P$: C, 51.64; H, 5.78; N, 11.25. Found: C, 51.66; H, 5.61; N, 11.25. RP: −11.510 (589 nm, T = 19 °C, C = 0.9).

*(3S)-3-(4-Aminobutyl)-4-hydroxy-1-[(4-hydroxy-2-phenylphenyl)methyl]-4-oxo-1,4-azaphosphinane-3-carboxylic Acid (**28c**).* White solid; yield 76% (0.78 g, 1.083 mmol). ^{1}H NMR (D_2O, 400 MHZ): δ ppm 7.54−7.44 (m, 3H), 7.54−7.44 (m, 1H), 7.34 (d, 2H), 6.97 (dd, 1H), 6.86 (df, 1H), 4.34/4.19 (2d, 2H), 3.33−3.05 (2m, 2H), 3.19−2.78 (2m, 2H), 2.95 (m, 2H), 2.07−1.63 (2m, 2H), 1.85−1.35 (2m, 2H), 1.59 (m, 2H), 1.2−1 (2m, 2H). HRMS: calcd for $[M + H]^+$ 433.1888; found, 433.1888. Elemental Anal. Calcd (%) for $C_{22}H_{29}N_2O_5P$: C, 61.10; H, 6.76; N, 6.48. Found: C, 60.81; H, 6.31; N, 6.49.

*(3S)-3-(4-Aminobutyl)-1-[[4-chloro-2-(4-chlorophenyl)-phenyl]-methyl]-4-hydroxy-4-oxo-1,4-azaphosphinane-3-carboxylic Acid (**28d**).* White solid; yield 66% (0.267 g, 0.55 mmol). ^{1}H NMR (D_2O, 400 MHZ): δ ppm 7.55−7.5 (2d, 2H), 7.5 (d, 2H), 7.4 (d, 1H), 7.28 (d, 2H), 4.3 (dd, 2H), 3.35−3.05 (2m, 2H), 3.15−2.8 (2m, 2H), 2.9 (m, 2H), 2.05−1.65 (2m, 2H), 1.8−1.3 (2m, 2H), 1.55 (m, 2H), 1.05 (m, 2H). HRMS: calcd for $[M + H]^+$ 485.1159; found, 485.1172. Elemental Anal. Calcd (%) for $C_{22}H_{27}Cl_2N_2O_4P$: C, 54.44; H, 5.61; N, 5.77. Found: C, 55.11; H, 5.26; N, 5.87. RP: −17.410 (589 nm, T = 19 °C, C = 1.0).

*(3S)-3-(4-Aminobutyl)-1-[(4-fluoro-2-phenylphenyl)-methyl]-4-hydroxy-4-oxo-1,4-azaphosphinane-3-carboxylic Acid (**28e**).* White solid; yield 41% (0.141 g, 0.324 mmol). ^{1}H NMR (D_2O, 300 MHZ): δ ppm 7.6 (dd, 1H), 7.49 (m, 3H), 7.34 (m, 2H), 7.22 (td, 1H), 7.15 (dd, 1H), 4.31 (AB, 2H), 3.32−3.06 (2m, 2H), 3.16−2.8 (2m, 2H), 2.92 (m, 2H), 2.05−1.6 (2m, 2H), 1.82−1.33 (2m, 2H), 1.56 (m, 2H), 1.07 (m, 2H) | NMR ^{19}F (D_2O, 300 MHZ): δ ppm −111.5. HRMS: calcd for $[M + H]^+$ 435.1845; found, 435.1842. Elemental Anal. Calcd (%) for $C_{22}H_{28}FN_2O_4P$: C, 60.82; H, 6.50; N, 6.45. Found: C, 60.79; H, 6.07; N, 6.19.

*(3S)-3-(4-Aminobutyl)-1-[(4-fluoro-2-phenylphenyl)-methyl]-4-hydroxy-4-oxo-1,4-azaphosphinane-3-carboxylic Acid (**28f**).* White solid; yield 72% (0.348 g, 0.797 mmol). ^{1}H NMR (D_2O, 300 MHZ): δ ppm 7.6 (dd, 1H), 7.49 (m, 3H), 7.34 (m, 2H), 7.22 (td, 1H), 7.15 (dd, 1H), 4.31 (AB, 2H), 3.32−3.06 (2m, 2H), 3.16−2.8 (2m, 2H), 2.92 (m, 2H), 2.05−1.6 (2m, 2H), 1.82−1.33 (2m, 2H), 1.56 (m, 2H), 1.07 (m, 2H). ^{19}F NMR: (D_2O, 300 MHZ): δ ppm −111.5. HRMS: calcd for $[M + H]^+$ 437.1750; found, 437.1754. Elemental Anal. Calcd (%) for $C_{20}H_{26}FN_4O_4P$: C, 60.82; H, 6.50; N, 6.45. Found: C, 60.82; H, 6.07; N, 6.19.

*(3S)-3-(4-Aminobutyl)-1-[(4-fluoro-2-pyrimidin-5-ylphenyl)-methyl]-4-hydroxy-4-oxo-1,4-azaphosphinane-3-carboxylic Acid (**28g**).* White solid; yield 86% (2.7 g, 6.02 mmol). ^{1}H NMR (D_2O, 400 MHZ): δ ppm 7.61 (dd, 1H), 7.36 (d, 2H), 7.26 (d, 2H), 7.23 (td, 1H), 7.15 (dd, 1H), 4.41/4.26 (2*d, 2H), 3.35−3.09 (m, 2H), 3.17−2.81 (m, 2H), 2.95 (m, 2H), 2.37 (s, 3H), 2.08−1.64 (m, 2H), 1.85−1.35 (m, 2H), 1.6 (m, 2H), 1.13−1.05 (m, 2H). HRMS: calcd for $[M + H]^+$ 449.2001; found, 449.2005. Elemental Anal. Calcd (%) for $C_{23}H_{30}FN_2O_4P$: C, 61.60; H, 6.74; N, 6.25. Found: C, 61.57; H, 6.53; N, 6.45. RP: −15.640 (589 nm, T = 20 °C, C = 1.0).

*(3S)-3-(4-Aminobutyl)-1-[[4-fluoro-2-(4-methoxyphenyl)-phenyl]methyl]-4-hydroxy-4-oxo-1,4-azaphosphinane-3-carboxylic Acid (**28h**).* White solid; yield 84% (0.492 g, 1.059 mmol). ^{1}H NMR (D_2O, 300 MHZ): δ ppm 7.57 (dd, 1H), 7.3 (d, 2H), 7.19 (td, 1H), 7.12 (dd, 1H), 7.08 (d, 2H), 4.32 (AB, 2H), 3.84 (s, 3H), 3.33−3.07 (2m, 2H), 3.13−2.8 (2m, 2H), 2.92 (m, 2H), 2.05−1.62 (2m, 2H), 1.83−1.32 (2m, 2H), 1.57 (m, 2H), 1.05 (m, 2H). HRMS: calcd for $[M + H]^+$ 465.1950; found, 465.1960. Elemental Anal. Calcd (%) for $C_{23}H_{30}FN_2O_5P$: C, 59.48; H, 651; N, 6.03. Found: C, 59.41; H, 6.76; N, 6.09. RP: −15.640 (589 nm, T = 20 °C, C = 1.0).

*(3S)-3-(4-Aminobutyl)-1-[[2-fluoro-6-(4-methoxyphenyl)-phenyl]methyl]-4-hydroxy-4-oxo-1,4-azaphosphinane-3-carboxylic Acid (**28i**).* White solid; yield 74% (0.240 g, 0.517 mmol). ^{1}H NMR (D_2O, 300 MHZ): δ ppm 7.54 (m, 1H), 7.3 (d, 2H), 7.28 (m, 1H), 7.21 (d, 1H), 7.11 (d, 2H), 4.42 (dd, 2H), 3.86 (s, 3H), 3.46−3.09 (m, 2H), 3.2−2.9 (m, 2H), 2.95 (m, 2H), 2.11−1.67 (m, 2H), 1.87−1.37 (m, 2H), 1.6 (m, 2H), 1.11 (m, 2H). HRMS: calcd for $[M + H]^+$ 465.1950; found, 465.1955. Elemental Anal. Calcd (%) for $C_{23}H_{30}FN_2O_5P$: C, 59.48; H, 6.51; N, 6.03. Found: C, 59.31; H, 6.75; N, 6.10.

*(3S)-3-(4-Aminobutyl)-1-[[2-(3,4-dimethoxyphenyl)-4-fluorophenyl]methyl]-4-hydroxy-4-oxo-1,4-azaphosphinane-3-carboxylic Acid (**28j**).* White solid; yield 87% (0.235 g, 0.475 mmol). ^{1}H NMR (D_2O, 300 MHZ): δ ppm 7.6 (dd, 1H), 7.2 (td, 1H), 7.1 (m, 1H), 7 (dd, 1H), 6.9 (dd, 1H), 4.4/4.25 (2 d, 2H), 3.8 (2 s, 6H), 3.35 (m, 1H), 3.2−2.75 (m, 5H), 2.05 (m, 1H), 1.8 (m, 1H), 1.6 (m, 3H), 1.3 (m, 1H), 1 (m, 2H). HRMS: calcd for $[M + H]^+$ 495.2056; found, 495.2056. Elemental Anal. Calcd (%) for $C_{24}H_{32}FN_2O_6P$: C, 58.29; H, 6.52; N, 5.67. Found: C, 58.64; H, 6.44; N, 5.72. RP: −23.170 (589 nm, T = 21 °C, C = 0.8).

*(3S)-3-(4-Aminobutyl)-1-[4-fluoro-2-(1-methyl-1H-imidazole-5-yl)benzyl]-4-hydroxy-4-oxo-1,4-azaphosphinane-3-carboxylic Acid (**28k**).* White solid; yield 72% (6.1g, 13.913 mmol). ^{1}H NMR (D_2O, 400 MHZ): δ ppm 7.8 (s, 1H), 7.68 (dd, 1H), 7.33 (td, 1H), 7.22 (dd, 1H), 7.1 (s, 1H), 4.25/4.18 (AB, 2H), 3.6−3.2 (2m, 2H), 3.45 (s, 3H), 3.3−3 (2m, 2H), 2.95 (m, 2H), 2.12−1.71 (2m, 2H), 1.9−1.42 (2m, 2H), 1.6 (m, 2H), 1.3−1 (m, 2H).^{19}F NMR: (D_2O, 400

https://doi.org/10.1021/acs.jmedchem.0c02072
J. Med. Chem. 2021, 64, 3897−3910

MHZ): δ ppm −109.75. HRMS: calcd for $[M + H]^+$ 439.1906; found, 439.1905. Elemental Anal. Calcd (%) for $C_{20}H_{28}FN_4O_4P$: C, 54.79; H, 6.44; N, 12.78. Found: C, 54.41; H, 6.12; N, 12.74. RP: −27.720 (589 nm, T = 20 °C, C = 0.7).

*(3S)-3-(4-Aminobutyl)-4-hydroxy-1-[[2-(4-methylphenyl)-phenyl]methyl]-4-oxo-1,4-azaphosphinane-3-carboxylic Acid (**28l**).* White solid; yield 68% (0.272 g, 0.632 mmol). ^{1}H NMR (D_2O, 400 MHZ): δ ppm 7.6−7.35 (m, 4H), 7.33−7.22 (2d, 4H), 4.33 (AB, 2H), 3.19−2.8 (2m, 2H), 2.91 (m, 2H), 2.35 (s, 3H), 2.06−1.58 (2m, 2H), 1.82−1.32 (2m, 2H), 1.57 (m, 2H), 1.07 (m, 2H). HRMS: calcd for $[M + H]^+$ 431.2095; found, 431.2097. Elemental Anal. Calcd (%) for $C_{23}H_{31}N_2O_4P$: C, 64.17; H, 7.26; N, 6.51. Found: C, 64.03; H, 6.92; N, 6.45. RP: −13.150 (589 nm, T = 20 °C, C = 0.9).

*(3S)-3-(4-Aminobutyl)-4-hydroxy-4-oxo-1-[[2-(2-oxo-1H-pyridin-4-yl)phenyl]methyl]-1,4-azaphosphinane-3-carboxylic Acid (**28m**).* White solid; yield 84% (0.321 g, 0.741 mmol). ^{1}H NMR (D_2O, 300 MHZ): δ ppm 7.65−7.3 (m, 4H), 7.6 (d, 1H), 6.55 (s, 1H), 6.5 (d, 1H), 4.35 (dd, 2H), 3.5 (2m, 2H), 3.25−2.9 (2m, 2H), 2.9 (m, 2H), 2.15−1.7 (2m, 2H), 1.85−1.4 (2m, 2H), 1.6 (m, 2H), 1.1 (m, 2H). MS HRMS: calcd for $[M + H]^+$ 434.1841; found, 434.1838. Elemental Anal. Calcd (%) for $C_{21}H_{28}N_3O_5P$: C, 58.19; H, 6.51; N, 9.69. Found: C, 58.88; H, 6.31; N, 9.95. RP: −10.530 (589 nm, T = 19 °C, C = 1.0).

*(3S)-3-(4-Aminobutyl)-1-[[4-fluoro-2-(2-oxo-1H-pyridin-4-yl)-phenyl]-methyl]-4-hydroxy-4-oxo-1,4-azaphosphinane-3-carboxylic Acid (**28n**).* White solid; yield 86% (0.480 g, 1.063 mmol). ^{1}H NMR (D_2O, 400 MHZ): δ ppm 7.64 (dd, 1H), 7.62 (d, 1H), 7.29 (td, 1H), 7.18 (dd, 1H), 6.57 (d, 1H), 6.53 (dd, 1H), 4.3 (dd, 2H), 3.51−3.15 (2m, 2H), 3.24−2.95 (2m, 2H), 2.92 (m, 2H), 2.13−1.7 (2m, 2H), 1.86−1.38 (2m, 2H), 1.58 (m, 2H), 1.1 (m, 2H). ^{19}F NMR: (D_2O, 400 MHZ): δ ppm −109.6. HRMS: calcd for $[M + H]^+$ 452.1746; found, 452.1745. Elemental Anal. Calcd (%) for $C_{21}H_{27}FN_3O_5P$: C, 55.87; H, 6.03; N, 9.31. Found: C, 56.06; H, 5.96; N, 9.21. RP: −10.270 (589 nm, T = 19 °C, C = 0.9).

*(3S)-3-(4-Aminobutyl)-1-[[4-fluoro-2-(6-methoxypyridin-3-yl)-phenyl]methyl]-4-hydroxy-4-oxo-1,4-azaphosphinane-3-carboxylic Acid (**28o**).* White solid; yield 73% (0.306 g, 0.657 mmol). ^{1}H NMR (D_2O, 400 MHZ): δ ppm 8.2 (d, 1H), 7.6 (dd, 1H), 7.3 (td, 1H), 7.2 (dd, 1H), 7.0 (dd, 1H), 6.9 (s, 1H), 4.3 (dd, 2H), 3.9 (s, 3H), 3.4−3.1 (2m, 2H), 3.2−2.8 (2m, 2H), 2.95 (m, 2H), 2.1−1.7 (2m, 2H), 1.85−1.35 (2m, 2H), 1.6 (m, 2H), 1.07 (m, 2H). HRMS: calcd for $[M + H]^+$ 466.1903; found, 466.1903. Elemental Anal. Calcd (%) for $C_{22}H_{29}FN_3O_5P$: C, 56.77; H, 6.28; N, 9.03. Found: C, 57.18; H, 6.17; N, 9.05. RP: −11.850 (589 nm, T = 20 °C, C = 0.9).

*(3S)-3-(4-Aminobutyl)-1-[[2-(2,3-dimethylimidazol-4-yl)-phenyl]-methyl]-4-hydroxy-4-oxo-1,4-azaphosphinane-3-carboxylic Acid (**28p**).* White solid; yield 35% (0.157 g, 0.361 mmol). ^{1}H NMR (D_2O, 400 MHZ): δ ppm 7.75−7.45 (m, 4H), 7.45 (s, 1H), 4.25 (m, 2H), 3.5−3.2 (2m, 2H), 3.4−3.1 (m, 2H), 3.4 (s, 3H), 2.9 (m, 2H), 2.65 (s, 3H), 2.1−1.7 (2m, 2H), 1.9−1.45 (2m, 2H), 1.6 (m, 2H), 1.25−1.1 (2m, 2H). HRMS: calcd for $[M + H]^+$ 435.2157; found, 435.2179. Elemental Anal. Calcd (%) for $C_{21}H_{31}N_4O_4P$: C, 50.37; H, 5.88; N, 10.21. Found: C, 49.57; H, 5.92; N, 9.92. RP: −23.310 (589 nm, T = 20 °C, C = 0.9).

*(3S)-3-(4-Aminobutyl)-1-[2-(1,2-dimethyl-1H-imidazole-5-yl)-4-fluorobenzyl]-4-hydroxy-4-oxo-1,4-azaphosphinane-3-carboxylic Acid (**28q**).* White solid; yield 56% (0.2 g, 0.442 mmol). ^{1}H NMR (D_2O, 400 MHZ): δ ppm 7.75 (dd, 1H), 7.55 (s, 1H), 7.5 (m, 1H), 7.3 (dd, 1H), 4.25 (s, 2H), 3.55 (m, 1H), 3.45 (s, 3H), 3.4 (m, 1H), 3.25 (m, 1H), 3.15 (dd, 1H), 2.95 (t, 2H), 2.65 (s, 3H), 2.15 (m, 1H), 1.9 (m, 1H), 1.75 (m, 1H), 1.65 (m, 2H), 1.45 (m, 1H), 1.3 (m, a1H), 1.15 (m, 1H). HRMS: calcd for $[M + H]^+$ 453.2063; found, 453.2058. Elemental Anal. Calcd (%) for $C_{21}H_{30}FN_4O_4P$: C, 47.29; H, 5.86; N, 10.50. Found: C, 46.18; H, 5.24; N, 10.02. RP: −28.200 (589 nm, T = 20 °C, C = 0.9).

*(3S)-3-(4-Aminobutyl)-1-[(4-fluoro-2-pyridin-3-ylphenyl)-methyl]-4-hydroxy-4-oxo-1,4-azaphosphinane-3-carboxylic Acid (**28r**).* White solid; yield 82% (0.303 g, 0.696 mmol). ^{1}H NMR (D_2O, 300 MHZ): δ ppm 8.62 (dd, 1H), 8.54 (d, 1H), 7.89 (dt, 1H), 7.7 (dd, 1H), 7.6 (dd, 1H), 7.34 (td, 1H), 7.23 (dd, 1H), 4.35 (m, 2H), 3.46−3.12 (2m, 2H), 3.18−2.87 (2m, 2H), 2.97 (m, 2H), 2.12−1.67 (2m, 2H), 1.88−1.37 (2m, 2H), 1.61 (m, 2H), 1.11 (m, 2H). ^{19}F NMR: (D_2O, 300 MHZ): δ ppm −111). HRMS: calcd for $[M + H]^+$ 436.1797; found, 436.1794. Elemental Anal. Calcd (%) for $C_{21}H_{27}FN_3O_4P$: C, 57.93; H, 6.25; N, 9.65. Found: C, 57.69; H, 5.69; N, 9.60. RP: −19.680 (589 nm, T = 20 °C, C = 0.9).

*(3S)-3-(4-Aminobutyl)-1-[[2-(4-chlorophenyl)-4-fluoro-phenyl]-methyl]-4-hydroxy-4-oxo-1,4-azaphosphinane-3-carboxylic Acid (**28s**).* White solid; yield 90% (0.374 g, 0.798 mmol). ^{1}H NMR (D_2O, 400 MHZ): δ ppm 7.62 (dd, 1H), 7.54 (d, 2H), 7.35 (d, 2H), 7.25 (td, 1H), 7.17 (dd, 1H), 4.39/4.28 (2d, 2H), 3.4−3.09 (2m, 2H), 3.13−2.84 (2m, 2H), 2.95 (m, 2H), 2.09−1.65 (2m, 2H), 1.86−1.36 (2m, 2H), 1.6 (m, 2H), 1.09 (m, 2H). HRMS: calcd for $[M + H]^+$ 469.1455; found, 469.1452. Elemental Anal. Calcd (%) for $C_{21}H_{27}FN_3O_4P$: C, 56.35; H, 5.80; N, 5.97. Found: C, 56.19; H, 5.57; N, 5.97. RP: −12.560 (589 nm, T = 20 °C, C = 0.9).

Pharmacology Materials and Methods. *IC_{50} Evaluation on Human TAFIa.* Human TAFI (4 nM, Calbiochem) was incubated with human thrombin (10 nM, Sigma) and human thrombomodulin (5 nM, American Diagnostica) in the presence of calcium (10 mM). After incubation for 20 min, the activation reaction was stopped by addition of PPACK (1 μM final), an irreversible thrombin inhibitor. The reactions took place in Hepes buffer (25 mM Hepes, 137 mM NaCl, 3.5 mM KCl) + 0.1% bovine albumin, pH = 7.4 at 28 °C and with stirring. The test compound was added to the solution of TAFIa (2 nM) and incubated for 45 min in the presence of hippuryl-arginine (5 mM). The reaction was stopped by addition of hydrochloric acid (1 M) neutralized subsequently with sodium hydroxide (1 M), and then the mixture was buffered with disodium hydroxyphosphate (1 M pH = 7.4). The reaction product—hippuric acid—was revealed by addition of cyanuric chloride (6%). The reaction mixture was stirred (vortex) and then centrifuged. The supernatant was transferred to a 96-well microplate, and the absorbance was measured using a spectrophotometer at 405 nm (Spectramax plus, Molecular Devices). The OD value of a well containing the reagents without TAFI was subtracted from all the measured OD values. The percentage inhibition of TAFIa at a given concentration of the tested compound was determined by means of the following formula: % inhibition = 100 − [(OD compound × 100)/OD carrier]. Data were analyzed according to a one-phase exponential decay function to evaluate IC_{50} (n = 2/compound).

Ki Evaluation on Human TAFIa, CPN, and CPB. All the reactions were performed at 25 °C in Hepes buffer (hepes 25 mM, NaCl 137 mM, KCl 3.5 mM) + 0.1% bovine serum albumin at pH = 7.4 and under stirring. Human pancreatic CPB (2 nM, Sigma) and **28k** (0, 2.5, 5, 10 μM) or human plasma CPN (20 nM, Elastin Product Company) and **28k** (0, 100, 200, 400 μM) or activated TAFI (as previously described) and **28k** (0, 1, 2, 4 nM) were mixed in the presence of different concentrations of hippuryl-Arginine (from 0.1 to 12 mM, Sigma). The reaction was performed for 25 (for CPB and CPN) or 45 min (for TAFIa) at 25 °C, then stopped by addition of HCl (1 M), and then neutralized by addition of sodium hydroxide (1 M). The reaction was then buffered by addition of di-sodium hydroxyphosphate (1 M, pH = 7.4). Hippuric acid was detected by addition of cyanuric chloride. After centrifugation (13,200 rpm), the supernatant was recovered and transferred in a 96-well plate. The absorbance (405 nm) of the wells without CPB or CPN (blank) was subtracted to samples for each concentration of the substrate. The calculation of Ki (n = 5) was evaluated by the method of apparent Km.[23,24]

Animals. Experiments were performed on adult male Sprague Dawley (SD) or Wistar rats (Charles River). All experiments were conducted in accordance with local ethical laws and local ethics committees in accordance with the French regulations (Decree n° 2013-118 from 01 February 2013 relative to the protection of animals used for scientific purposes and 4 orders of 01 February 2013).

In Vitro Fibrinolytic Activity of Compounds by Thrombo-Elastometry (TE) on SD Rat Blood. Fresh rat whole blood (480 μL) was preincubated for 2 min at 37 °C with 0.8 μM or different concentrations of compounds (500 μL final) in a plastic cup. A mixture of 20 μL of $CaCl_2$ (0.2M, starTEM, ROTEM) and 20 μL of

https://doi.org/10.1021/acs.jmedchem.0c02072
J. Med. Chem. 2021, 64, 3897−3910

tissue factor (ex-TEM, ROTEM) was then added. Human tPA [16 nM, (Alteplase, Boehringer Ingelheim)] was added, and the cups were placed in the rotational thromboelastometer (ROTEM). ROTEM continuously records viscoelastic profiles of blood clot formation/dissolution by measuring the viscoelastic changes by a pin which oscillates into the blood. Fibrin formation and fibrinolysis were followed for 3 h at 37 °C. The clot firmness was measured as the area under the curve (AUC) of the amplitude in function of time (thrombo-elastogram). The AUC was computed using the trapezoid rule (software GraphPad Prism 5). The percentage of inhibition of AUC (*vs* vehicle) was evaluated for 0.8 μM of compounds, n = 2/compound. For dose response experiments, the concentration which decreases by 50% the AUC ("EC_{50}") was calculated (n = 1−5).

Ex Vivo Fibrinolytic Activity of Compounds by TE in Rat. Experiments were performed on adult male SD rats (350−450 g). Rats were anesthetized [ketamine (75 mg/kg IP) (Merial)/xylazine (5 mg/kg IP) (Bayer Healthcare)] and maintained anesthetized all along the experiment by an IV infusion (ketamine 50 mg/kg/h, xylazine 3 mg/kg/h). The corporal temperature was maintained by a thermo-regulated coverage. Catheters were placed in jugular veins and tail vein (for anesthesia and treatments). Rats were treated with vehicle (0.9% NaCl) or compounds (0.6 mg/kg). The treatments were administered IV. Thirty and 60 min after IV treatment, arterial blood (from carotid artery) was collected on sodium citrate. For 0.5 mL of blood, 20 μL of $CaCl_2$ (0.2M, starTEM, ROTEM), 20 μL of tissue factor (ex-TEM, ROTEM), and 16 nM of tPA (Alteplase, Boehringer Ingelheim) were mixed in a cup. The cups were placed in the rotational thromboelastometer (ROTEM). Fibrin formation and fibrinolysis were followed for 1 h at 37 °C. The AUC was calculated for each condition (software GraphPad Prism 5). The percentage of inhibition (*vs* AUC of group vehicle) was then calculated at 30 and/or 60 min post IV treatment (n = 1−2/compound).

Structure Determination. X-ray structure determinations were performed following methods described[25] (PDB entry 3D68, 7NEE and 7NEU) and are further described in the associated content section.

■ ASSOCIATED CONTENT

Supporting Information

The Supporting Information is available free of charge at https://pubs.acs.org/doi/10.1021/acs.jmedchem.0c02072.

Molecular formula strings of TAFIa inhibitors (CSV)

General synthetic procedures, characterizations of key compounds, ^{1}H NMR spectra, molecular formula strings, chiral separation procedure, ADME and pharmacokinetic data, protein production, crystallization conditions, X-ray diffraction data and docking protocol (PDF)

Atomic coordinates of TAFIa **8a** (PDB)

Atomic coordinates of TAFIa **14d** (PDB)

■ AUTHOR INFORMATION

Corresponding Author

Arnaud-Pierre Schaffner − *Institut de Recherches Servier, 92150 Suresnes, France;* orcid.org/0000-0002-2848-6554; Phone: +33-6 02 06 63 91; Email: arnaud-pierre.schaffner@servier.com

Authors

Patricia Sansilvestri-Morel − *Institut de Recherches Servier, 92150 Suresnes, France*

Nicole Despaux − *Institut de Recherches Servier, 92150 Suresnes, France*

Elisabeth Ruano − *Institut de Recherches Servier, 92150 Suresnes, France*

Thierry Persigand − *Institut de Recherches Servier, 92150 Suresnes, France*

Alain Rupin − *Institut de Recherches Servier, 92150 Suresnes, France*

Philippe Mennecier − *Institut de Recherches Servier, 92150 Suresnes, France*

Marie-Odile Vallez − *Institut de Recherches Servier, 92150 Suresnes, France*

Eric Raimbaud − *Institut de Recherches Servier, 92150 Suresnes, France*

Patrice Desos − *Institut de Recherches Servier, 92150 Suresnes, France*

Philippe Gloanec − *Institut de Recherches Servier, 92150 Suresnes, France*

Complete contact information is available at: https://pubs.acs.org/10.1021/acs.jmedchem.0c02072

Notes

The authors declare no competing financial interest.

■ ACKNOWLEDGMENTS

The authors thank co-workers at the Analytical Division of the Institut de Recherches Servier for providing the detailed chemical analysis of the compounds, Philippe Baumy at Technology Servier for the DMPK experiments, Andras Kotschy and Laurent-Michel Vuillard for their advices in preparing the manuscript.

■ ABBREVIATIONS

A, apical; ADME, absorption, distribution, metabolism, elimination; AUC, area under curve; B, basal; br s, broad signal; *n*-BuLi, *n*-butyllithium; CLp, plasma clearance; CLr, renal clearance; CP, carboxypeptidase; DBC, dibenzyl carbonate; DMF, *N*,*N*-dimethylformamide; DMSO, dimethyl sulfoxide; EC_{50}, half maximal effective concentration; ER, efflux ratio; Fabs, prediction of oral absorption; fu, fraction unbound; h, hour; hep, hepatocyte; hu, human; IC_{50}, half maximal inhibitory concentration; inhib, inhibition; IP, intraperitoneal; IV, intravenous; Ki, inhibition constant; Km, Michaelis constant; m, mouse; MF, metabolic bioavailability; mic, microsome; min, minute; mp, melting point; OD, optical density; Papp, apparent permeability coefficient; PK, Pharmacokinetics; PPACK, Hippuryl-D-phenylalanyl-L-prolyl-L-arginine chloromethyl ketone; r, rat; rpm, rotation per minute; rt, room temperature; SD, sprague dawley; SEM, standard error of mean; TAFIa, activated thrombin activatable fibrinolysis inhibitor; TE, thromboelastometry; THF, tetrahydrofuran; TMSBr, trimethylsilyl bromide; tPA, tissue plasminogen activator; $t_{1/2}$, terminal half-life; Vss, apparent volume of distribution at steady state

■ REFERENCES

(1) George, M.; Fareed, J.; Van Thiel, D. H. Low levels of thrombin activatable fibrinolysis inhibitor (TAFI) in patients with chronic liver disease. *Thromb. Haemostasis* **2001**, *85*, 667−670.

(2) Eichinger, S.; Schönauer, V.; Weltermann, A.; Minar, E.; Bialonczyk, C.; Hirschl, M.; Schneider, B.; Quehenberger, P.; Kyrle, P. A. Thrombin-activatable fibrinolysis inhibitor and the risk for recurrent venous thromboembolism. *Blood* **2004**, *103*, 3773−3776.

(3) da Cunha, V.; Vincelette, J.; Zhao, L.; Nagashima, M.; Kawai, K.; Yuan, S.; Emayan, K.; Islam, I.; Hosoya, J.; Sullivan, M. E.; Dole, W. P.; Morser, J.; Buckman, B. O.; Vergona, R.; Wang, Y.-X. A novel inhibitor of activated thrombin activatable fibrinolysis inhibitor

(TAFIa) - part II: enhancement of both exogenous and endogenous fibrinolysis in animal models of thrombosis. *Thromb. Haemostasis* **2007**, *97*, 54−61.
(4) Vercauteren, E.; Peeters, M.; Hoylaerts, M. F.; Lijnen, H. R.; Meijers, J. C. M.; Declerck, P. J.; Gils, A. The hyperfibrinolytic state of mice with combined thrombin-activatable fibrinolysis inhibitor (TAFI) and plasminogen activator inhibitor-1 gene deficiency is critically dependent on TAFI deficiency. *J. Thromb. Haemostasis* **2012**, *10*, 2555−2562.
(5) Swaisgood, C. M.; Schmitt, D.; Eaton, D.; Plow, E. F. In vivo regulation of plasminogen function by plasma carboxypeptidase B. *J. Clin. Invest.* **2002**, *110*, 1275−1282.
(6) Noguchi, K.; Edo, N.; Miyoshi, N.; Isobe, A.; Watanabe, A.; Ito, Y.; Morishima, Y.; Yamaguchi, K. Fibrinolytic potential of DS-1040, a novel orally available inhibitor of activated thrombin-activatable fibrinolysis inhibitor (TAFIa). *Thromb. Res.* **2018**, *168*, 96−101.
(7) Nantermet, P. G.; Barrow, J. C.; Lindsley, S. R.; Young, M.; Mao, S.-S.; Carroll, S.; Bailey, C.; Bosserman, M.; Colussi, D.; McMasters, D. R.; Vacca, J. P.; Selnick, H. G. Imidazole acetic acid TAFIa inhibitors: SAR studies centered around the basic P 1 ′ group. *Bioorg. Med. Chem. Lett.* **2004**, *14*, 2141−2145.
(8) (a) Barrow, J. C.; Nantermet, P. G.; Stauffer, S. R.; Ngo, P. L.; Steinbeiser, M. A.; Mao, S.-S.; Carroll, S. S.; Bailey, C.; Colussi, D.; Bosserman, M.; Burlein, C.; Cook, J. J.; Sitko, G.; Tiller, P. R.; Miller-Stein, C. M.; Rose, M.; McMasters, D. R.; Vacca, J. P.; Selnick, H. G. Synthesis and evaluation of imidazole acetic acid inhibitors of activated thrombin-activatable fibrinolysis inhibitor as novel antithrombotics. *J. Med. Chem.* **2003**, *46*, 5294−5297. (b) Bunnage, M. E.; Blagg, J.; Steele, J.; Owen, D. R.; Allerton, C.; McElroy, A. B.; Miller, D.; Ringer, T.; Butcher, K.; Beaumont, K.; Evans, K.; Gray, A. J.; Holland, S. J.; Feeder, N.; Moore, R. S.; Brown, D. G. Discovery of Potent & Selective Inhibitors of Activated Thrombin-Activatable Fibrinolysis Inhibitor for the Treatment of Thrombosis. *J. Med. Chem.* **2007**, *50*, 6095−6103.
(9) Polla, M. O.; Tottie, L.; Nordén, C.; Linschoten, M.; Müsil, D.; Trumpp-Kallmeyer, S.; Aukrust, I. R.; Ringom, R.; Holm, K. H.; Neset, S. M.; Sandberg, M.; Thurmond, J.; Yu, P.; Hategan, G.; Anderson, H. Design and synthesis of potent, orally active, inhibitors of carboxypeptidase U (TAFIa). *Med. Chem.* **2004**, *12*, 1151−1175.
(10) Do, Y. H.; Gifford-Moore, D. S.; Beight, D. W.; Rathnachalam, R.; Klimkowski, V. J.; Warshawsky, A. M.; Lu, D. Inhibition of thrombin activatable fibrinolysis inhibitor by cysteine derivatives. *Thromb. Res.* **2005**, *116*, 265−271.
(11) Islam, I.; Bryant, J.; May, K.; Mohan, R.; Yuan, S.; Kent, L.; Morser, J.; Zhao, L.; Vergona, R.; White, K.; Adler, M.; Whitlow, M.; Buckman, B. O. 3-Mercaptopropionic acids as efficacious inhibitors of activated thrombin activatable fibrinolysis inhibitor (TAFIa). *Bioorg. Med. Chem. Lett.* **2007**, *17*, 1349−1354.
(12) Brink, M.; Dahlén, A.; Olsson, T.; Polla, M.; Svensson, T. Design and synthesis of conformationally restricted inhibitors of active thrombin activatable fibrinolysis inhibitor (TAFIa). *Med. Chem.* **2014**, *22*, 2261−2268.
(13) Yoshimoto, N.; Sasaki, T.; Sugimoto, K.; Ishii, H.; Yamamoto, K. Design and characterization of a selenium-containing inhibitor of activated thrombin-activatable fibrinolysis inhibitor (TAFIa), a zinc-containing metalloprotease. *J. Med. Chem.* **2012**, *55*, 7696−7705.
(14) Zhao, L.; Nagashima, M.; Vincelette, J.; Sukovich, D.; Li, W.; Subramanyam, B.; Yuan, S.; Emayan, K.; Islam, I.; Hrvatin, P.; Bryant, J.; Light, D. R.; Vergona, R.; Morser, J.; Buckman, B. O.; Wang, Y.-X. A novel inhibitor of activated thrombin-activatable fibrinolysis inhibitor (TAFIa)—Part I: Pharmacological characterization. *J. Thromb. Haemostasis* **2007**, *97*, 45−53.
(15) Adler, M.; Buckman, B.; Bryant, J.; Chang, Z.; Chu, K.; Emayan, K.; Hrvatin, P.; Islam, I.; Morser, J.; Sukovich, D.; West, C.; Yuan, S.; Whitlow, M. Structures of potent selective peptide mimetics bound to carboxypeptidase B. *Acta Crystallogr., Sect. D: Biol. Crystallogr.* **2008**, *64*, 149−157.
(16) Halland, N.; Czech, J.; Czechtizky, W.; Evers, A.; Follmann, M.; Kohlmann, M.; Schreuder, H. A.; Kallus, C. Sulfamide as zinc binding motif in small molecule inhibitors of activated thrombin activatable fibrinolysis inhibitor (TAFIa). *J. Med. Chem.* **2016**, *59*, 9567−9573.
(17) Halland, N.; Brönstrup, M.; Czech, J.; Czechtizky, W.; Evers, A.; Follmann, M.; Kohlmann, M.; Schiell, M.; Kurz, M.; Schreuder, H. A.; Kallus, C. Novel small molecule inhibitors of activated thrombin activatable fibrinolysis inhibitor (TAFIa) from natural product anabaenopeptin. *J. Med. Chem.* **2015**, *58*, 4839−4844.
(18) Skidgel, R. A.; Erdös, E. G. Structure and function of human plasma carboxypeptidase N, the anaphylatoxin inactivator. *Int. Immunopharmacol.* **2007**, *7*, 1888−1899.
(19) Deprèle, S.; Montchamp, J.-L. Palladium-catalyzed hydrophosphinylation of alkenes and alkynes. *J. Am. Chem. Soc.* **2002**, *124*, 9386−9387.
(20) Dunne, K. S.; Bisaro, F.; Odell, B.; Paris, J.-M.; Gouverneur, V. Diastereoselective Ring-Closing Metathesis: Synthesis of P-Stereogenic Phosphinates from Prochiral Phosphinic Acid Derivatives. *J. Org. Chem.* **2005**, *70*, 10803−10809.
(21) Gloanec, P.; Schaffner, A.-P.; Sansilvestri-Morel, P.; Rupin, A.; Mennecier, P.; Vallez, M.-O. Novel Phosphinane and Azaphosphinane Derivatives, Method for Preparing Same and Pharmaceutical Compositions Containing Same. WO2017121969A1, 2017.
(22) Sansilvestri-Morel, P.; Bertin, F.; Lapret, I.; Neau, B.; Blanc-Guillemaud, V.; Petit-Dop, F.; Tupinon-Mathieu, I.; Delerive, P. S62798, a TAFIa inhibitor, accelerates endogenous thrombolysis in a murine model of pulmonary thromboembolism. *Eur. Heart J.* **2020**, *41*, No. ehaa946.3361.
(23) Kakkar, T.; Boxenbaum, H.; Mayersohn, M. Estimation of Ki in a competitive enzyme-inhibition model: comparisons among three methods of data analysis. *Drug Metab. Dispos.* **1999**, *27*, 756−762.
(24) Kakkar, T.; Pak, Y.; Mayersohn, M. Evaluation of a minimal experimental design for determination of enzyme kinetic parameters and inhibition mechanism. *J. Pharmacol. Exp. Ther.* **2000**, *293*, 861−869.
(25) Marx, P. F.; Brondijk, T. H. C.; Plug, T.; Romijn, R. A.; Hemrika, W.; Meijers, J. C. M.; Huizinga, E. G. Crystal structures of TAFI elucidate the inactivation mechanism of activated TAFI: a novel mechanism for enzyme autoregulation. *Blood* **2008**, *112*, 2803−2809.
(26) Jones, G.; Willett, P.; Glen, R. C.; Leach, A. R.; Taylor, R. Development and validation of a genetic algorithm for flexible docking 1 1Edited by F. E. Cohen. *J. Mol. Biol.* **1997**, *267*, 727−748.

https://doi.org/10.1021/acs.jmedchem.0c02072
J. Med. Chem. 2021, 64, 3897−3910